Laser Engineering

Kelin Kuhn
University of Washington

© 1998 by Prentice-Hall, Inc.
A Pearson Education Company
Upper Saddle River, NJ 07458

The author and publisher of this book have used their best efforts in preparing this book. These efforts include the development, research, and testing of the theories and programs to determine their effectiveness. The author and publisher make no warranty of any kind, expressed or implied, with regard to these programs or the documentation contained in this book. The author and publisher shall not be liable in any event for incedental or consequential damages in connection with, or arising out of, the furnishing, performance, or use of these programs.

Contents

iv

Contents

12

Other Major Commercial Lasers

Objectives

Carbon dioxide lasers

- To summarize the generic characteristics of the CO_2 laser.
- To describe the various energy states of the CO_2 laser and to summarize how these states interact with each other.
- To summarize the sequence of historical events leading to the development of the CO_2 laser.
- To describe the major characteristics of waveguide versus free space CO_2 lasers.
- To describe the construction of a commercial waveguide CO_2 laser.

Excimer lasers

- To summarize the generic characteristics of the excimer laser.
- To describe the various energy states of the excimer laser and to summarize how these states interact with each other.
- To summarize the sequence of historical events leading to the development of the excimer laser.
- To describe the general design principles underlying excimer lasers. These include preionization, corona discharge circuitry, and main discharge circuitry.
- To describe the construction of a commercial excimer laser.

Semiconductor diode lasers

- To summarize the sequence of historical events leading to the development of the semiconductor laser.
- To describe the energy band structure of the semiconductor diode laser.

- To summarize the process of pumping the semiconductor diode laser with a PN-junction.
- To describe the process of creating a semiconductor laser cavity by cleaving the semiconductor material.
- To describe the similarities and differences between homostructure and heterostructure semiconductor diode lasers.
- To describe the importance of vertical and horizontal confinement in designing semiconductor laser structures.
- To describe the major vertical and horizontal confinement structures.
- To describe the general physical principles governing the design of quantum wells, with special emphasis on the importance of the width of the quantum well in determining the optical properties of quantum well laser diodes.

12.1 THE DESIGN OF CARBON DIOXIDE LASERS

CO_2 lasers operate over a series of vibrational and rotational bands in the regions 9.4 and 10.6 μm. They are both high-average-power and high-efficiency laser systems. Commercially available cw CO_2 lasers range in power from 6 watts to 10,000 watts, and custom lasers are available at even higher powers. Small (2 to 3 feet long) CO_2 lasers can produce hundreds of watts of average power at an efficiency of 10%. Larger CO_2 lasers can produce many kilowatts of cw power. CO_2 lasers are widely used in such diverse commercial applications as marking of electronic components, wafers, and chips; marking on anodized aluminum; trophy engraving; acrylic sign making; rapid prototyping of 3D models; cutting of ceramics, textiles, and metals; carpet, sawblade, and sail cutting; drilling; thin film deposition; and wire stripping (see Figure 12.1). They find application in the medical field for laser surgery, and in research for spectroscopy and remote sensing. Military applications include imaging, mapping, and range-finding. They have also been used in inertial confinement fusion as an alternative to large glass lasers.

CO_2 is a laser material totally unlike the materials discussed so far in this text. Conventional lasers lase off of electronic transitions between various atomic states. CO_2 lasers lase off molecular transitions between the various vibrational and rotational states of CO_2. Among other things, this means that CO_2 lasers have a longer wavelength and higher efficiency than most conventional lasers. Additional information on CO_2 lasers can be found in Cheo,[1] Duley,[2] Tyte,[3] and Witteman.[4] Additional information on high peak power and gas dynamic CO_2 lasers can be found in Anderson,[5] Beaulieu,[6] and Losev.[7]

---

[1] Peter K. Cheo, *Handbook of Molecular Lasers* (New York: Marcel-Dekker Inc., 1987).

[2] W. W. Duley, *CO₂ Lasers: Effects and Applications*, (New York: Academic Press, 1976).

[3] D. C. Tyte, *Advances in Optical Electronics, Vol. 1*, ed D. W. Goodwin, (New York: Academic Press, 1970), pp. 129–198.

[4] W. J. Witteman, *The CO₂ laser* (Berlin: Springer-Verlag, 1987).

[5] John Anderson, *Gasdynamic Lasers: An Introduction* (New York: Academic Press, 1976).

[6] J. A. Beaulieu, *Proc. IEEE* 59:667 (1971).

[7] S. A. Losev, *Gasdynamic Laser* (Berlin: Springer-Verlag, 1981).
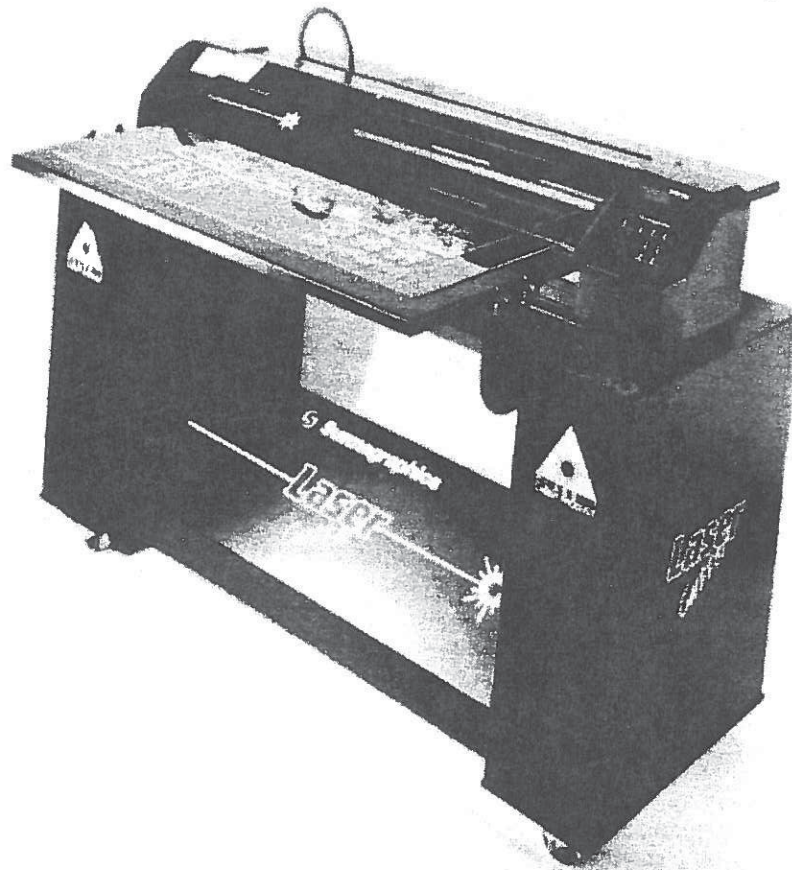
Figure 12.1 Carbon dioxide laser cutting system. (Courtesy of Synrad, Mukilteo, WA, and Summagraphics)

12.1.1 Introduction to CO_2 Laser States

Consider the CO_2 molecule as depicted in Figure 12.2. There are three normal modes of vibration possible in this molecule: the symmetric stretch mode, the bending mode, and the asymmetric stretch mode. The states are labeled by a notation (p_1, p_2, p_3) where the subscripts refer to the various normal modes and where p is an integer corresponding to the number of quanta in the mode. Thus (001) is the state with one quanta in the asymmetric stretch mode and (200) is the state with two quanta in the symmetric stretch mode. The total vibrational energy of the CO_2 molecule is expressed as

$$E(\nu_1, \nu_2, \nu_3) = h\nu_1 \left(p_1 + \frac{1}{2} \right) + h\nu_2 \left(p_2 + \frac{1}{2} \right) + h\nu_3 \left(p_3 + \frac{1}{2} \right) \qquad (12.1)$$

where ν_1, ν_2, ν_3 represent the frequencies of the particular modes.[8]

[8] Amnon Yariv, *Optical Electronics*, 4th ed. (Philadelphia, PA: Saunders College Publishing, 1991), p. 242.
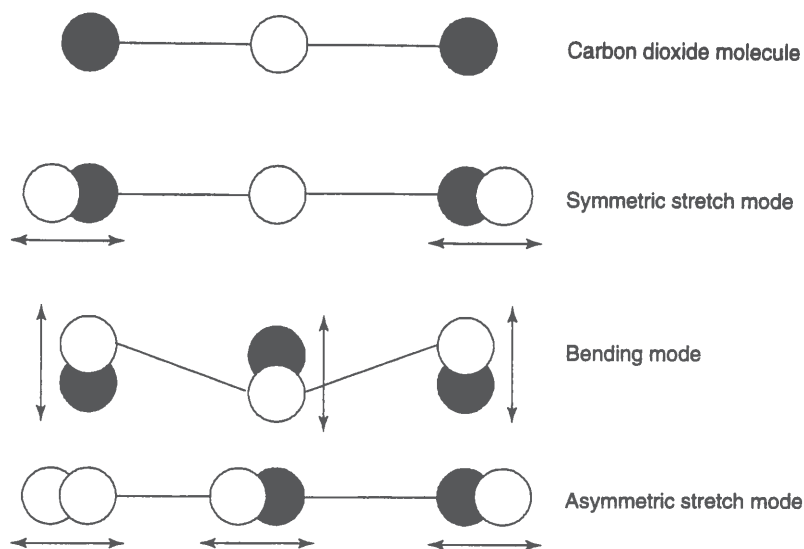
Figure 12.2 Normal modes of the carbon dioxide molecule.

The CO_2 molecules can also rotate, resulting in a series of closely spaced states characterized by the rotational quantum number J. The rotational energies of a given vibrational state i relative to the $J = 0$ level are given as

$$E_{i,J} = hc_o B_i J(J+1) - hc_o D J^2 (J+1)^2 \qquad (12.2)$$

where B_i and D are constants.[9]

The principal laser transitions in CO_2 are the (001) to (100) 10.6 μm transitions and the (001) to (020) 9.4 μm transitions (see Figure 12.3). Each of the levels (001), (100), and (020) consists of a series of rotational states. Transitions in CO_2 occur between states where $J_{odd} \rightarrow (J+1)_{even}$ (termed the P-branch) and $J_{odd} \rightarrow (J-1)_{even}$ (termed the R-branch). (See Figure 12.4.)

If no wavelength discrimination is provided in the cavity, the P-branch of the (001) to (100) 10.6 μm transition will dominate. However, if wavelength selection is provided (by a grating, for example), it is possible to lase on any of the allowed P- or R-branch transitions. Notice, however, that since both the (001)$\rightarrow$(100) and the (001)$\rightarrow$(020) transitions share the same upper laser level, then the (001)$\rightarrow$(100) transition must be suppressed for the (001)$\rightarrow$(100) transition to lase.

The majority of CO_2 lasers contain a mixture of three gases (CO_2, N_2, and He) in a roughly 0.8:1:7 ratio.[10] The CO_2 is the laser gain material. The N_2 has only one excited mode (the symmetrical stretch mode) and the energy of the (1) N_2 vibration nicely aligns with the (001) upper state of the CO_2 molecule (see Figure 12.3). Since the N_2 vibrational states are metastable (very long lifetimes) the energy in the (1) N_2 transition (plus a little kinetic energy) can be transferred to a CO_2 molecule as a means of populating the (001)

---

[9] Amnon Yariv, *Quantum Electronics*, 2d ed. (New York: John Wiley and Sons, 1975), p. 213, Appendix 3.

[10] W. W. Duley, *CO_2 Lasers: Effects and Applications* (New York: Academic Press, 1976), p. 16.
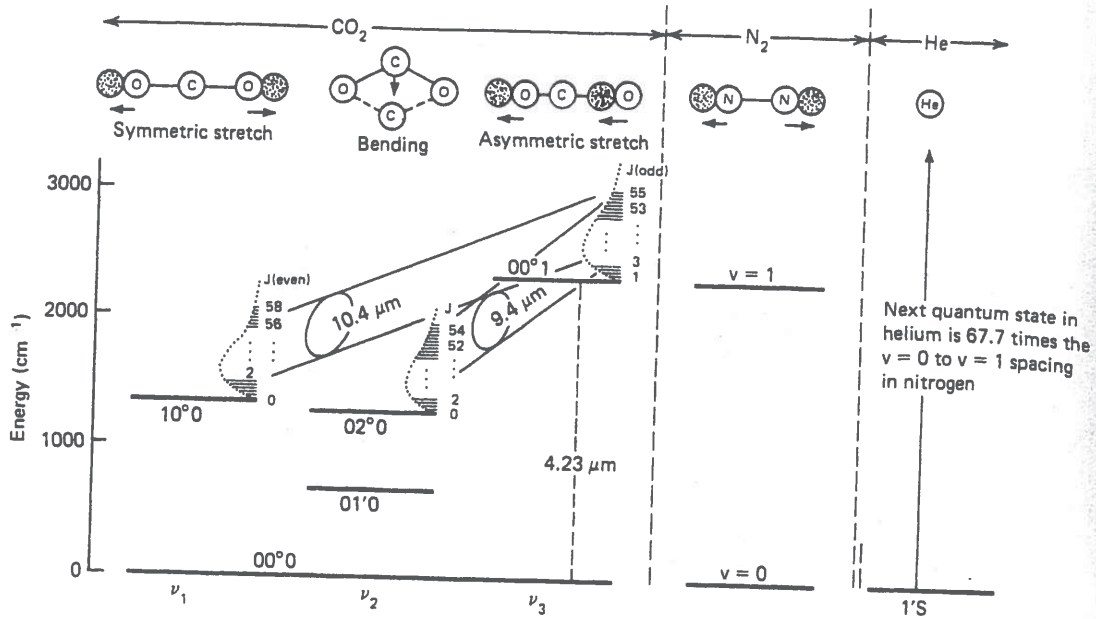
Figure 12.3   Laser states of the carbon dioxide molecule. (From LASER ELECTRONICS 2E. by VERDEYEN, J.T. ©1989, Figure 10.14, p. 336. Adapted by permission of Prentice-Hall, Inc., Upper Saddle River, NJ.)
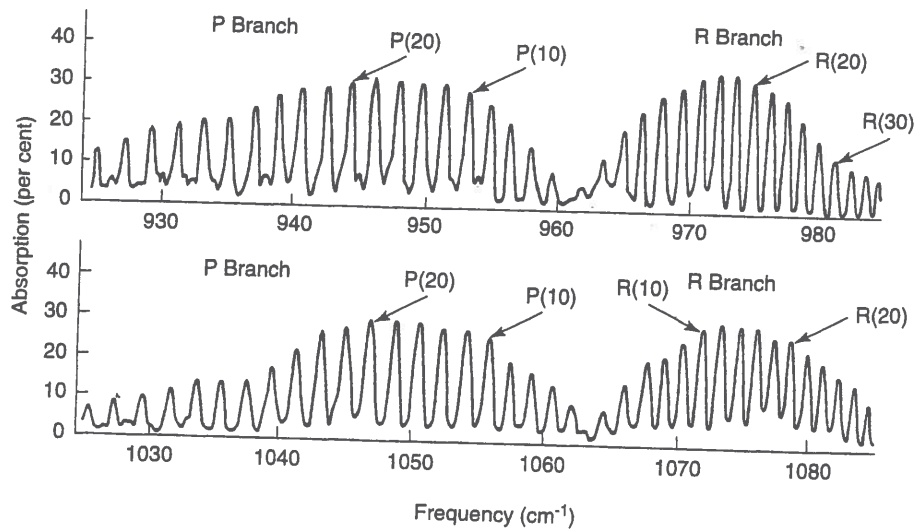
Figure 12.4   Absorption spectrum of the carbon dioxide molecule. (From E. F. Barker and A. Adel, *Phys. Rev.* 44:185 (1933))

upper CO_2 level (notice that the N_2–CO_2 energy transfer is very similar to the He–Ne energy transfer in HeNe lasers; see Section 9.1.3). The helium in the gas mixture provides cooling by means of thermal transfer to the walls (helium is a very thermally conductive gas). Helium also plays a role in optimizing the kinetic energy of the N_2 molecules for maximum energy transfer between the N_2 and CO_2.

Because of the metastable N_2 and the match between the (1) N_2 level and the (001) CO_2 level, the conversion efficiency between input electrical power to power in the upper laser state is 50 to 70%. Since the quantum efficiency is roughly 45%, this means that CO_2 lasers can operate at extremely high efficiencies (10 to 35%).

12.1.2 The Evolution of CO_2 Lasers

The first demonstration of laser action from CO_2 was reported by Patel in 1964.[11,12,13] The concept of using N_2 to transfer vibrational energy from the electrical discharge to the CO_2 was recognized by Legay and Legay-Sommaire in the same year[14] and the idea of incorporating helium for cooling was first proposed by Patel a year later.[15] During this period of rapid development on the CO_2 laser, Patel and other researchers were able to improve Patel's original 1 mW output to roughly 100 watts.[16,17,18]

The first CO_2 lasers were constructed from long tubes of glass where the desired laser mixture flowed through the glass tube (see Figure 12.5). Electrodes in the gas generated a plasma arc to excite the N_2 molecules into their symmetrical stretch mode. Although the very first demonstration of laser action from CO_2 used RF excitation, systems soon converted to DC excitation for increased power.[19]

The original glass tube CO_2 lasers operated at low pressures with the electrical discharge running longitudinally down the cavity. As a consequence, operating pressures were low due to the necessity to create and maintain a plasma over a long distance. However, in 1970, Beaulieu[20] first reported operation of an atmospheric pressure CO_2 laser by exciting the discharge transversely to the cavity (see Figure 12.6). These Transverse Excited Atmospheric (TEA) lasers offered higher gains and greater output powers than longitudinally excited lasers.

[11] C. K. N. Patel, *Phys. Rev. Lett.* 12:588 (1964).

[12] C. K. N. Patel, *Phys. Rev. Lett.* 13: 617 (1964).

[13] C. K. N. Patel, *Phys. Rev.* 136:A1187 (1964).

[14] F. Legay and N. Legay-Sommaire, *C. R. Acad. Sci.* 259B:99 (1964).

[15] C. K. N. Patel, P. K. Tien, and J. H. McFee, *Appl. Phys. Lett.* 7:290 (1965).

[16] C. K. N. Patel, *Phys. Rev.* 136:A1187 (1964).

[17] N. Legay-Sommaire, L. Henry, and F. Legay, *C.R. Acad. Sci.* 260B:3339 (1965).

[18] C. K. N. Patel, P. K. Tien, and J. H. McFee, *Appl. Phys. Lett.* 7:290 (1965).

[19] C. K. N. Patel, *Appl. Phys. Lett.* 7:15 (1965).

[20] A. J. Beaulieu, *Appl. Phys. Lett.* 16:504 (1970).
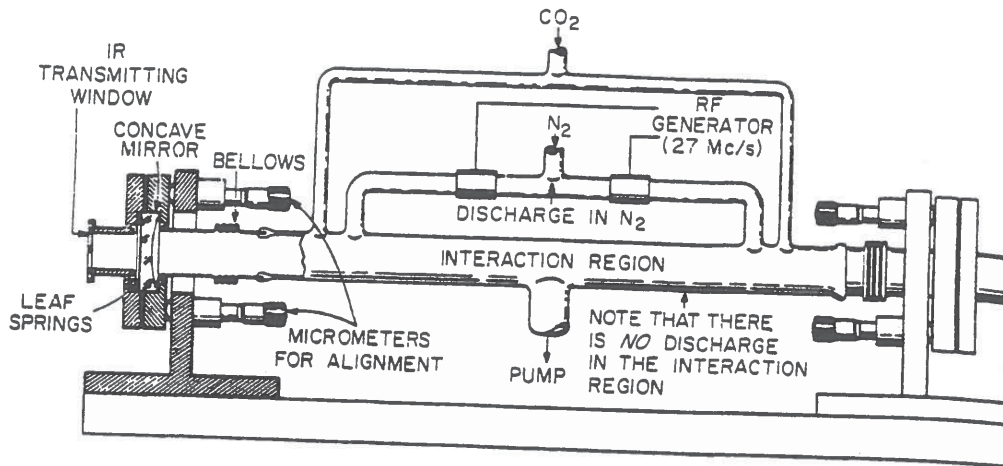
Figure 12.5 Early carbon dioxide laser construction. (From C. K. N. Patel, *Phys. Rev. Lett.* 13: 617 (1964). Reprinted with the permission of the author.)

The CO_2 laser Q-switches exceptionally well and Q-switched operation was reported in 1966 by a number of researchers including Flynn,[21,22] Kovacs,[23] Bridges,[24] and Patel.[25] However, the narrow bandwidth of CO_2 (approximately 50 MHz), means that physically long lasers are required to effectively demonstrate mode-locking. In spite of this difficulty, the first mode-locking of a conventional CO_2 laser was reported in 1968 by Caddes,[26] and Wood and Schwartz.[27] High-peak power can also be obtained from CO_2 lasers by pulsing or gain switching the lasers.[28] TEA lasers are especially well-suited for production of high-peak power CO_2 laser pulses.[29]

In a conventional CO_2 laser, the output power will increase as the gas flow is increased. This increased power is thought to be due to enhanced cooling and more effective removal of dissociation products such as CO and O_2 from the CO_2 discharge.[30] However, in many applications, it is not possible to support the peripheral equipment for handling flowing gases and a sealed laser configuration is required. In a sealed laser, the lack of gas flow means that some mechanism must be provided to regenerate the dissociated gas products

[21]G. W. Flynn, M. A. Kovacs, C. K. Rhodes, and A. Javan, *Appl. Phys. Lett.* 8:63 (1966).

[22]G. W. Flynn, L. O. Hocker, A. Javan, M. A. Kovacs, and C. K. Rhodes, *IEEE J. Quan. Elec.* QE-2:378 (1966).

[23]G. W. Flynn, L. O. Hocker, A. Javan, M. A. Kovacs, and C. K. Rhodes, *IEEE J. Quan. Elec.* QE-2:378 (1966).

[24]T. J. Bridges, *Appl. Phys. Lett.* 9:174 (1966).

[25]C. K. N. Patel, *Phys. Rev. Lett.* 16:613 (1966).

[26]D. E. Caddes, L. M. Osterink, and R. Targ, *Appl. Phys. Lett.* 12:74 (1968).

[27]O. R. Wood and S. E. Schwartz, *Appl. Phys. Lett.* 12:263 (1968).

[28]A. E. Hill, *Appl. Phys. Lett.* 12:324 (1968).

[29]W. W. Duley, *CO_2 Lasers: Effects and Applications* (New York: Academic Press, 1976), Chapter 2.

[30]Tyte, D. C., in *Advances in Optical Electronics*, Vol 1, ed D.W. Goodwin (New York: Academic Press, 1970), pp. 167–168.
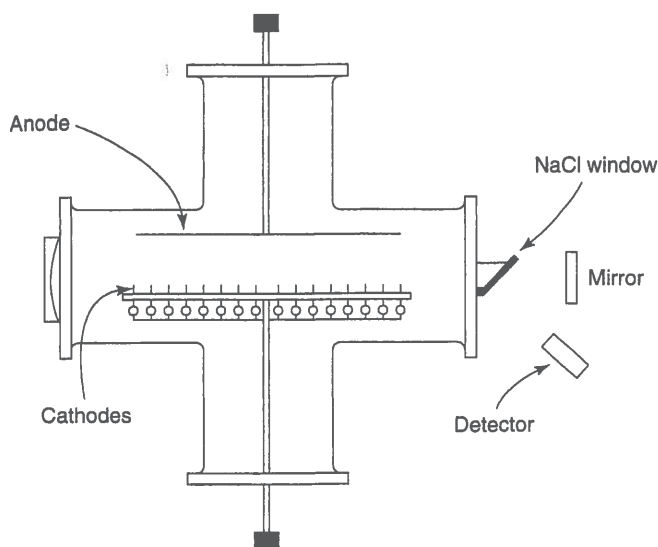
Figure 12.6   A schematic of an early Transverse Excited Atmospheric (TEA) laser. (Reprinted with permission from A. J. Beaulieu, *Appl. Phys. Lett.* 16:504 (1970). ©1970 American Institute of Physics.)

(particularly the oxygen species) back into CO_2. If these products are permitted to react with the tube walls, the chemical equilibrium of the plasma is disturbed and additional dissociation products are formed. Various regeneration methods include adding additional gases, periodically heating the tube, or incorporating catalyst alloys on the electrodes. Sealed lasers demonstrating such regeneration methods were first developed by Wittman in 1965[31] and further developed by Wittman[32] and Carbone.[33]

The initial use of flowing gases to improve the output performance of CO_2 lasers led to the development of another fascinating way to pump CO_2. The basic idea is to begin with a hot equilibrium gas mixture and then to expand the mixture through a supersonic nozzle. This lowers the temperature and pressure of the gas mixture in a time short compared to the upper state lifetime. When this occurs, the upper laser level cannot track with the temperature and pressure changes and so remains at its initial values. In contrast, the lower level population drops dramatically. The result is a population inversion that extends some distance downstream of the supersonic nozzle (see Figure 12.7). Lasers using this type of pumping are called gas dynamic lasers and were first suggested by Konyukhov and Prokhorov[34] in 1966 and demonstrated by Gerry[35] and Konyukhov.[36]

The most spectacular forms of gas dynamic lasers are those run using jet or rocket engines as the pump source. The basic idea is to create a laser gas mixture by burning some type of fuel that generates the CO_2. The fuel source is often ignited with a methanol burner,

---

[31]W. J. Witteman, *Phys. Lett.* 18:125 (1965).

[32]W. J. Witteman, *IEEE J. Quan. Electron.* QE-5:92 (1969).

[33]R. J. Carbone, *IEEE J. Quan. Electron.* QE-5:48 (1969).

[34]V. K. Konyukhov and A. M. Prokhorov, *JETP Lett.* 3:286 (1966).

[35]E. T. Gerry, *IEEE Spectrum* 7:51 (1970).

[36]V. K. Konyukhov, I. V. Matrosov, A. M. Prokhorov, D. T. Shalunov, and N. N. Shirokov, *JETP Lett.* 12:321 (1970).
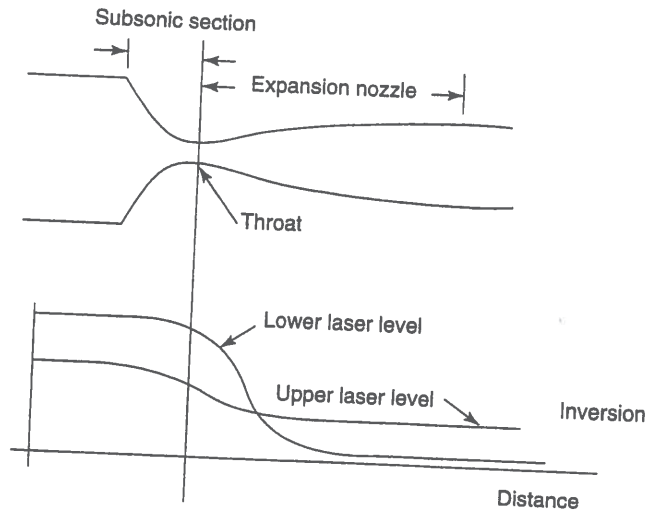
Figure 12.7 Gas dynamic lasers operate by creating a population inversion via gas expansion through a nozzle. (From E. T. Gerry, "Gasdynamic Lasers," *IEEE Spectrum* 7:51–58 (1970). ©1970 IEEE.)
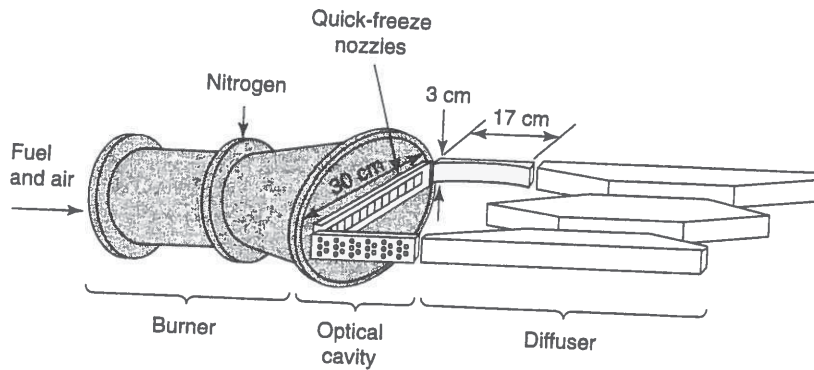
Figure 12.8 The most spectacular forms of gas dynamic lasers are those run using jet or rocket engines as the pump source. (From E. T. Gerry, *IEEE Spectrum* 7:51 (1970). ©1970 IEEE.)

which also injects water into the mixture. (The water is used to decrease the lifetime of the lower laser state.) Extra nitrogen is added to improve the excitation of the CO_2. The resulting mixture is then compressed by the engine and allowed to expand out through a series of supersonic nozzles. The optical cavity is then located sideways across the expansion chamber (see Figure 12.8).[37]

---

[37]E. T. Gerry, *IEEE Spectrum* 7:51 (1970).
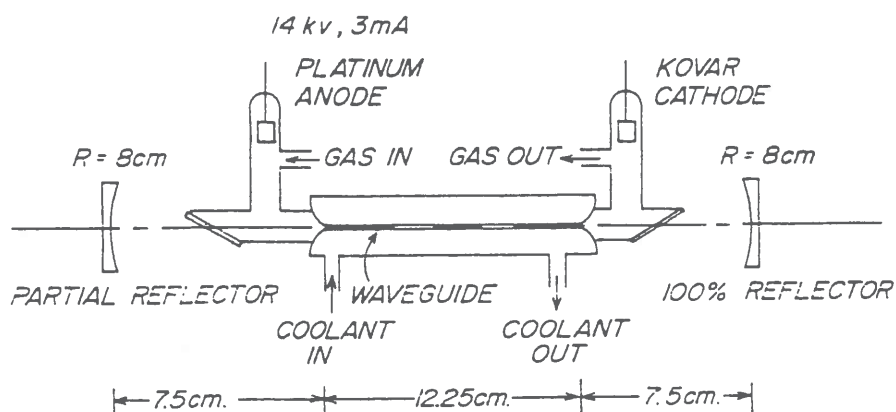
Figure 12.9   The construction of an early waveguide carbon dioxide laser. (Reprinted with permission from T. J. Bridges, E. G. Burkhardt, and P. W. Smith, *Appl. Phys. Lett.* 20:403 (1972). ©1972 American Institute of Physics.)

12.1.3 Waveguide CO_2 Lasers

One very good method for improving CO_2 laser performance is to decrease the bore size of the laser. This increases the number of gas collisions with the bore and significantly enhances the cooling rate (see Figure 12.9). If the electrodes are located transversely (rather than longitudinally) in the laser cavity, then the possibility also exists of using the electrodes themselves as an optical waveguide, thus permitting an even smaller bore size. The use of such a waveguide allows increased gas pressure with the attendant advantages of improved gain and larger linewidth. Operation in a waveguide mode also offers some additional advantages in alignment stability. The concept of a waveguide CO_2 laser was first proposed in 1964 by Marcatili and Schmeltzer[38] and later demonstrated by Steffen and Kneubuhl[39] and Smith.[40] Transverse-excited waveguide lasers are disclosed by Smith in U.S. Patent #3,815,047.[41]

Waveguide lasers use a small bore to confine the laser beam. The bore is itself an optical element, composed of two or four optically reflecting walls. Conventional mirrors are placed on either end of the cavity, but (unlike a conventional free space laser) these mirrors do not define a Gaussian beam in the cavity. Instead, the laser establishes various stable modes inside the bore (not unlike the modes in a laser fiber or a zig-zag slab laser). It is also possible to control the mode formation by introducing artifacts inside the bore that force the development of stable reflecting points.[42]

---

[38] E. A. J. Marcatili and R. A. Schmeltzer, *Bell Sys. Tech. J.* 43:1783 (1964).

[39] H. Steffen and F. K. Kneubuhl, *Phys. Lett.* 27A:612 (1968).

[40] P. W. Smith, *Appl. Phys. Lett.* 19:132 (1971).

[41] Peter W. Smith, "Transversely Excited Waveguide Gas Laser," U.S. Patent #3,815,047, June 4, 1974.

[42] Peter Laakmann, "Sealed Off RF-Excited Gas Lasers and a Method for Their Manufacture," U.S. Patent #5,065,405, November 12, 1991.

Waveguide lasers are typically differentiated from free space lasers by a number called the Fresnel number. This is defined as

$$F = \frac{a^2}{L\lambda_o}$$

(12.3)

where a is the beam radius (for a cylindrical laser) or 1/2 the beam width (for a square laser), L is the length, and λ_o the free space wavelength. A laser with a Fresnel number of less than 0.5 is a true waveguide laser. A laser with a Fresnel number of greater than about 10 is a true free space laser. Lasers with Fresnel numbers around 1 are intermediate lasers that have some of the features of both classes.[43]

Waveguide lasers are typically smaller, lighter, easier to align, and cheaper than their glass tube ancestors. They also have significantly lower operating voltages, as the gas discharge must only be sustained transversely across the bore (a few millimeters) rather than longitudinally along the tube (many centimeters).

12.1.4 A Typical Modern CO_2 Industrial Laser

The remainder of this chapter will focus on a family of sealed low-power CO_2 lasers representative of modern commercial lasers used for industrial laser machining applications such as cutting and marking (see Figure 12.10). The specific units under discussion are the very popular series 48 sealed CO_2 lasers manufactured by Synrad in Mukilteo, Washington, U.S.A. These lasers represent an excellent example of modular design and are available in three power levels (10W, 25W, and 50W). (See Figure 12.11.)

CO_2 lasers can be operated with flowing gases or in a sealed configuration. Sealed lasers (such as the series 48 lasers) have obvious advantages in the industrial workplace as they do not require complex gas handling systems. Sealed lasers are only commercially available up to approximately 250 watts. The cross-over point between sealed laser technology and flowing gases technology is roughly 1 kW, and driven primarily by size and manufacturing constraints.[44]

Water-cooling is another critical issue in CO_2 laser design. Although CO_2 lasers are exceptionally efficient, 10% efficiency still means that 90% of the input power ends up somewhere else, usually as heat in the chassis. If the laser gets too hot, then the lower state population increases, and the laser performance drops. With good heat sink design, sealed CO_2 lasers can be operated in air-cooled mode up to approximately 25 watts. Past that power level, water-cooling is typically required.[45]

Design and manufacture of the series 48 module.   The basic series 48 module is described in U.S. Patent #5,065,405 (Peter Laakmann, "Sealed Off RF-Excited Gas Lasers and a Method for Their Manufacture," November 12, 1991) and the technology is discussed in U.S. Patent #4,805,182 (Peter Laakmann, "RF-Excited All-Metal Gas laser," February 14,

---

[43]Peter Laakmann, "Sealed Off RF-Excited Gas Lasers and a Method for Their Manufacture," U.S. Patent #5,065,405, November 12, 1991.

[44]Peter Laakmann, "Using Low Power CO_2 Lasers in Industrial Applications," Synrad Application Note.

[45]Peter Laakmann, "Using Low Power CO_2 Lasers in Industrial Applications," Synrad Application Note.
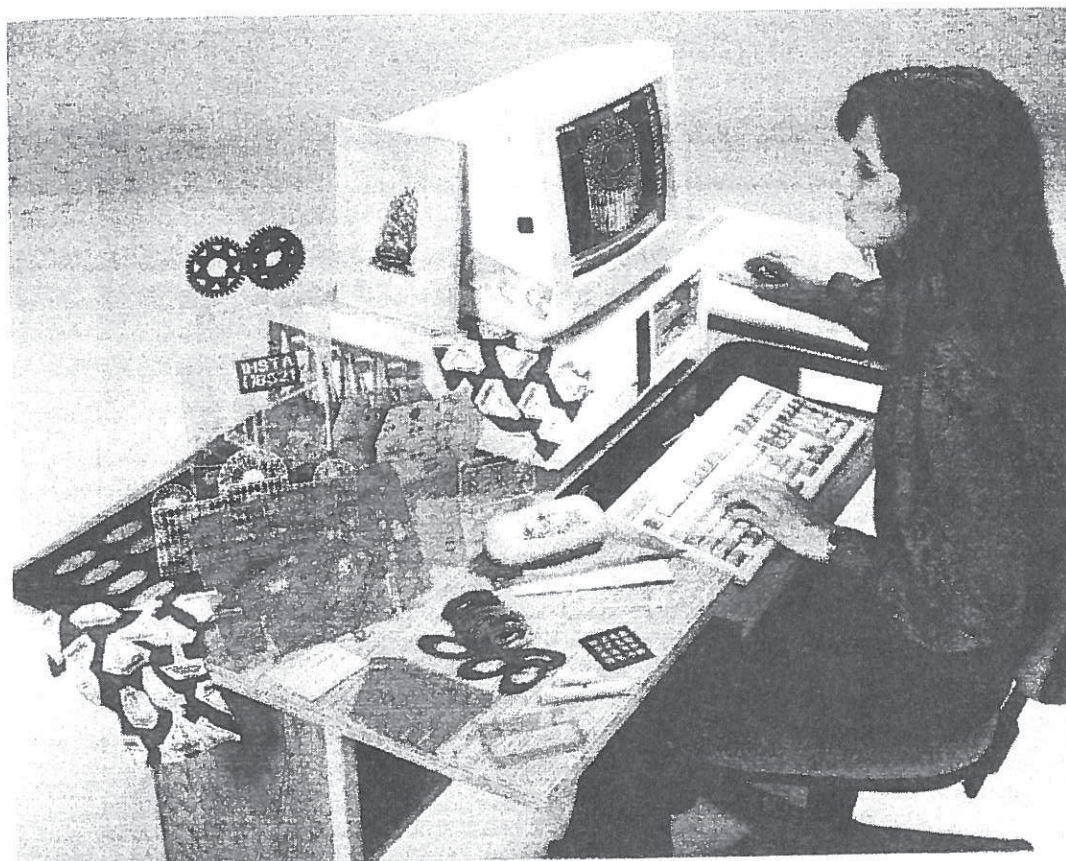
Figure 12.10   Typical products marked by a carbon dioxide laser. (Courtesy of Synrad)

1989). The key points of the design and manufacturing are described below and additional details may be found in the patents.

The basic series 48 module consists of two extruded aluminum electrodes and two extruded aluminum ground plane strips (see Figure 12.12). The inner surfaces of the electrodes and ground strips are optically reflective at 10.6 μm. (The electrodes are typically anodized with a 5 μm hard anodization to improve discharge stability and RF breakdown characteristics.[46]) The top and bottom electrodes are identical and measure approximately 1 cm by 2 cm by 40 cm long. The left and right ground plane strips are also identical and measure approximately 2 cm by 4 cm by 40 cm long. To reduce costs, the overall shape of the electrodes and ground planes is predefined by the extrusion process and only minor post-extrusion machining operations need to be performed.

The inner surfaces of the electrodes and the ground strips define the optical cavity of the laser. The bore of this cavity measures roughly 5 mm square, which gives the overall

---

[46]Y. F. Zhang, S. R. Byron, P. Laakmann, and W. B. Bridges, *Cleo '94*, 1994; *Tech. Digest Series*, Vol. 8, 94CH3463-7, pp. 358–9.
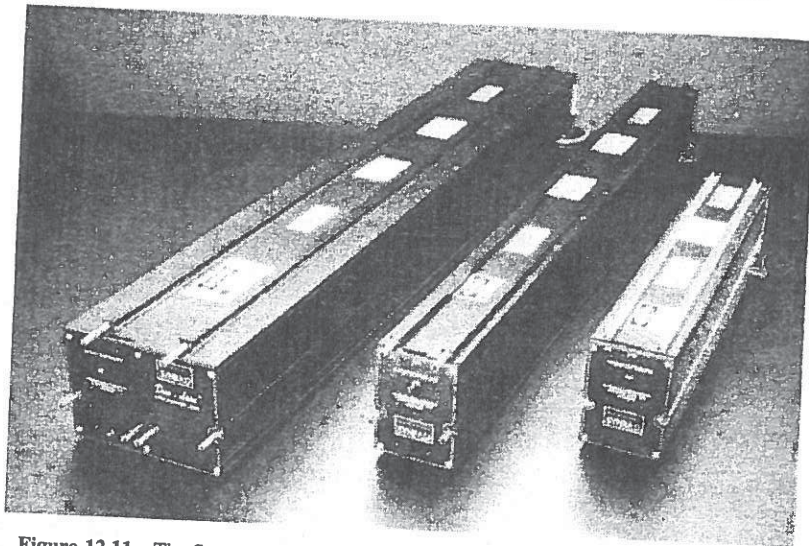
Figure 12.11 The Synrad series 48 sealed carbon dioxide lasers. (Courtesy of Synrad)
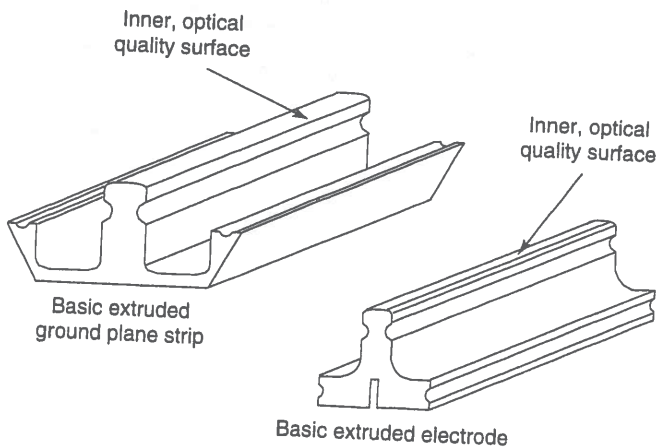
Figure 12.12 The Synrad electrodes and ground plane strips.

laser system a Fresnel number of approximately 1.5 and a diameter to length ratio of approximately 0.015. Thus, the laser operates in the intermediate regime between full waveguide operation and full free space operation. In this intermediate regime, only a fraction of the power of the optical wave interacts with the walls of the cavity. This fraction is high enough to obtain a good optical fill factor, but not so high as to create large losses due to absorption in the optical cavity structure.

If the optical surfaces of the electrodes and the ground strips are perfectly flat and aligned, then spurious reflections from the surfaces may cause aberrations in the output mode pattern. By deliberately introducing artifacts into the cavity geometry, these aberrations may be reduced or eliminated. Two types of artifacts have been found to be successful in reducing mode aberrations. The first artifact consists of slightly tapering the walls of the bore. In this method, the bore is made slightly larger near the end mirror than at the
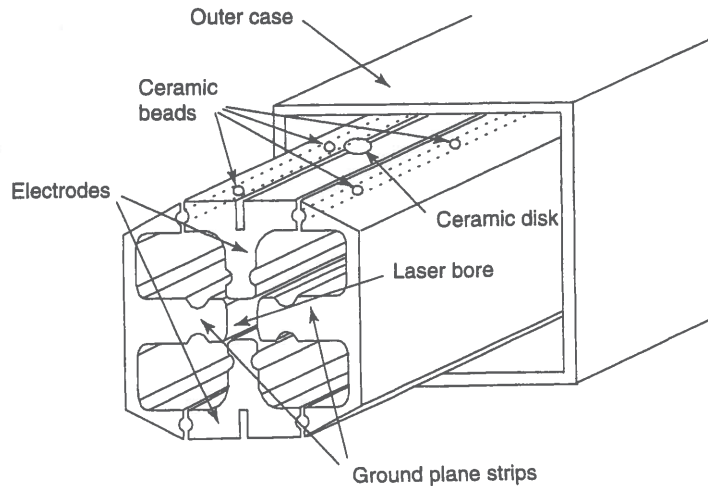
Figure 12.13   The Synrad series 48 cross-section.

front mirror. The taper angle is quite small, typically less than a milliradian. The second artifact consists of introducing small, sharp bends in the optical surfaces. The bends can be in one electrode and its adjacent ground strip, or in two opposing electrodes (or ground strips). If the bend is introduced into the electrode and its adjacent ground strip, then it is a bend on the order of 5 to 10 milliradians. If the bend is introduced into opposing electrodes (or ground strips), then it is on the order of 1 milliradian. These bends prevent reflections off all four walls from adding in phase to produce competing modes and parasitic oscillations.

The two electrodes and two ground planes are assembled in a clean room. The electrodes and ground plane strips are slipped into an outer case as shown in Figure 12.13. Small ceramic beads are used to isolate the electrodes from the ground plane strips. Larger ceramic disks are used to isolate the electrodes from the outer case. Electrical feedthroughs (which also serve as gas fill ports) are provided in the outer case.

A common cause of short lifetimes in CO_2 lasers is the accumulation of water vapor. Water vapor can migrate through the o-ring mirror seals, or be formed by hydrogen combining with dissociated oxygen. An effective way to minimize contamination due to water vapor is to introduce a getter into the cavity. A molecular sieve getter for removal of water vapor is typically inserted into the cavity during the initial assembly. Following the initial assembly, aluminum mirror mounts are welded to both ends of the tube. The laser module is then subjected to a high vacuum bake-out process. This process removes water as well as the majority of volatile contaminants such as hydrocarbons and hydrogen.

The bake-out process is followed by a passivation process where the laser module is exposed to an oxygen-helium plasma. The passivation process produces numerous oxygen species that react with the exposed aluminum parts and create aluminum oxides. (Al_2O_3, sapphire, is one of the many aluminum oxides formed by this process.) These oxides serve to

prevent oxygen loss in the finished laser and extend the operating lifetime. The passivation process also serves to clean the bore of the laser and prevent contamination of the mirrors during operation.

The passivation is performed by generating an oxygen plasma within the laser bore. To create all the oxides necessary for effective passivation, the plasma is operated at several different temperatures, and at peak excitation powers that exceed those the laser will experience in operation.

After the passivation is complete, the laser mirrors are added to the module. Although nearly perfect mirror alignment is required for effective operation of a true waveguide laser, the best mode quality and output power performance of an intermediate regime laser is often obtained when the end mirrors are aligned slightly off-axis. The back mirror is a 100% dielectric coating on silicon (3 meter concave for the 10 watt series 48 laser). The front mirror is flat with a partially reflective dielectric coating on ZnSe (95% reflectivity for the 10 watt series 48 laser). The mirrors are mounted against an o-ring seal and three small screws provide alignment adjustment. (Although the o-ring seal at first glance seems like a potentially unsatisfactory element, Synrad experience has shown them to work quite well. The leak rate is approximately 1 cm^3 of helium per year, not the limiting factor in the laser lifetime. The o-ring mounts do not fail catastrophically, and provide a simple and straightforward means to make alignment adjustments.[47])

Once the mirrors have been installed, the laser is again subjected to a short vacuum bake-out. This bake removes water vapor introduced by the mirror mounting operation. The bake is relatively short (120°C for 8 hours for the 10 watt series 48 laser) to avoid damaging the passivation layer.

Once the bake-out is completed, the laser is carefully realigned and permanently filled with the operating gas mixture. The operating mixture consists of roughly 7% xenon, 10% CO_2, 13% N_2, and 67% He.[48] (The xenon is added to lower the overall electron temperature and improve the cross-section of the (1) transition in N_2).[49] The basic laser module is now complete.

The finished laser module can be mounted in one of several different housings. The most common is to mount the laser in a simple housing incorporating an integral heat exchanger. The laser tube fits in the bottom of the housing, and the RF electronics to drive the electrodes mounts in the top (see Figure 12.14).

Expanding the basic module.
The basic 10 watt laser is designed to effectively scale to higher powers. Two electrodes, two ground strips, and an RF driver define a 10 watt module. Four electrodes (of the same length as the 10 watt electrodes), two ground strips (twice as long as the 10 watt ground strips), and two RF modules define the 25 watt module.

The two 25 watt modules are combined together in a simple but effective way to form the 50 watt module. The standard 25 watt module lases with its polarization vector

[47]P. Laakmann, *Lasers and Optronics* March: 35–41 (1989)

[48]P. Laakmann, "Using Low Power CO_2 Lasers in Industrial Applications," Synrad Application Note.

[49]W. J. Witteman, *The CO_2 Laser* (Berlin: Springer-Verlag, 1987), pp. 74–75.
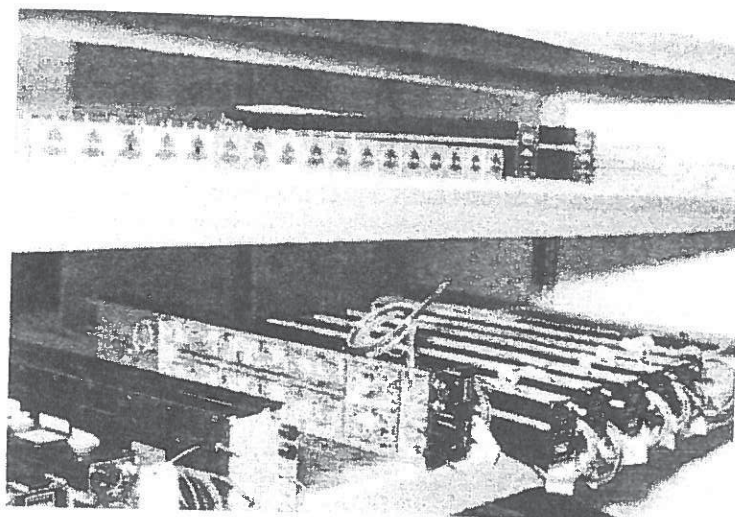
Figure 12.14   Synrad CO_2 series 48 internal modules and housings.   (Courtesy of Synrad)

25 watt module oriented with horizontal polarization

25 watt module oriented with vertical polarization

Element is transmissive for horizontal polarization, reflective for vertical polarization

Mirrors
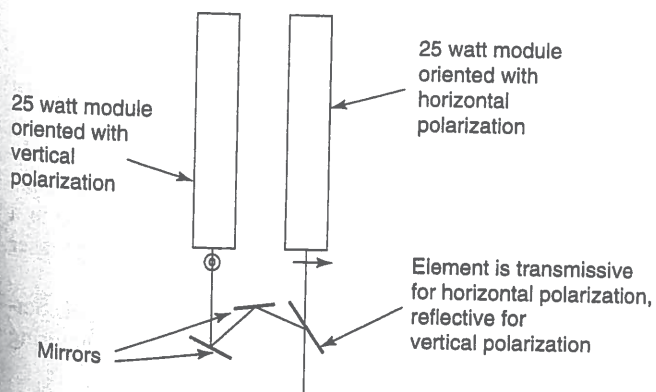
Figure 12.15   Combining the 25 watt beams together for the 50 watt unit.

parallel to the ground planes.[50]   If one 25 watt module is installed with its polarization vector vertical, and the second installed with its polarization vector horizontal, then the orthogonally polarized beams can be combined at the output using a polarizing beam splitter (see Figure 12.15).

The same modular scaling strategies are applied to the RF drive electronics.   The single 10 watt module uses one RF driver board. The 25 watt module uses two identical driver boards, and the 50 watt module uses four identical driver boards.

---

[50]Y. F. Zhang, S. R. Byron, P. Laakmann, and W. B. Bridges, *Cleo '94*, 1994; *Tech. Digest Series*, Vol. 8, 94CH3463-7, pp. 358-9.

**Design of the RF driver board.**   Although the very early CO_2 lasers frequently used a radio frequency (RF) discharge,[51,52,53,54,55] this was considered by most researchers to be an inefficient and inconvenient excitation source.[56] It was not until 1977, when Katherine Laakmann began re-examining the use of RF-excitation for waveguide lasers,[57] that the potential value of RF-excitation for small sealed waveguide lasers became apparent.

Conventional CO_2 lasers use a longitudinal high voltage DC current to create the plasma. In a DC longitudinally excited laser, the output power is difficult to control electrically. Changing the voltage across the electrodes changes the character of the plasma. This, in turn, alters the plasma impedance and the ability of the plasma to excite the CO_2 molecules. Thus, a rather small change in the exciting voltage can result in large changes in the laser performance. Furthermore, the length and stability characteristics of the longitudinal excitation make rapid changes in the laser performance difficult.

In the late seventies, Laakmann Electro-optics (started by Peter and Katherine Laakmann) developed the transverse RF-excited CO_2 laser. The major advantage of transverse RF-excited lasers is that the output power can be electrically controlled over a wide range, at rates of up to 20 kHz. (Figure 12.16 illustrates the control of the output power by alteration of the duty cycle for 5 kHz and 20 kHz operation from a 65 watt Synrad CO_2 laser.) Other advantages of RF-excitation include significantly lower voltages (hundreds compared to thousands of volts) and the possibility of longer laser lifetimes due to reductions in gas-dissociation-related damage.

RF-excitation does have its costs. In particular, transistor controlled RF-excited devices have roughly half the wallplug efficiency of similar DC-excited units.[58] Additionally, the power supplies required for RF-excitation are typically more expensive than those in an equivalent DC-excited unit.

The excitation frequency of the RF discharge ranges from a value of approximately $v/2a$ to $50v/a$, where a is the width of the laser bore, and v is the drift velocity of electrons in the laser gas. The drift velocity ranges from approximately $5 \cdot 10^6$ to $1 \cdot 10^7$ cm/sec in a typical CO_2 laser gas mixture.[59] Thus, for a typical transversely excited RF discharge laser system, appropriate excitation frequencies lie in the UHF-VHF region.

In order to avoid radio interference with other services, certain ISM (Industrial, Scientific, Military) frequencies have been set aside by the FCC for industrial uses requiring

---

[51]C. K. N. Patel, *Phys. Rev.* 136:A1187 (1964).

[52]P. Barchewitz, L. Dorbec, R. Farrenq, A. Truffert, and P. Vautier, *C. R. Hebd. Seanc. Acad. Sci.* 260:3581 (1965).

[53]P. Barchewitz, L. Dorbec, A. Truffert, and P. Vautier, *C. R. Hebd. Seanc. Acad. Sci.* 260:5491 (1965).

[54]R. Farrenq, C. Meyer, C. Rossetti, L. Dorbec, and P. Barchewitz, *C. R. Hebd. Seanc. Acad. Sci.* 261:2617 (1965).

[55]C. Rossetti, R. Farrenq, and P. Barchewitz, *J. Chim. Phys.* 64:93 (1967).

[56]Tyte, D. C., in *Advances in Optical Electronics*, Vol. 1, ed D. W. Goodwin (New York: Academic Press, 1970), p. 172.

[57]Katherine Laakmann, "Waveguide Gas Laser with High Frequency Transverse Discharge Excitation," U.S. Patent #4,169,251, September 25, 1979.

[58]P. Laakmann, *Lasers and Optronics* (1989), pp. 35–41.

[59]Katherine Laakmann, "Waveguide Gas Laser with High Frequency Transverse Discharge Excitation," U.S. Patent #4,169,251, September 25, 1979.
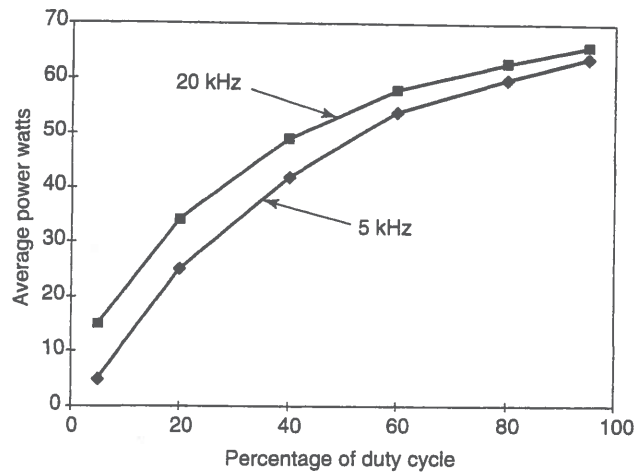
Figure 12.16   Output power versus duty cycle for the 57G Synrad laser. (Courtesy of Synrad)

large amounts of RF power. These ISM frequencies are used for larger RF CO_2 lasers and are 27.12 MHz and 40.68 MHz. Smaller lasers may operate outside of the ISM frequency limits if the shielding is sufficiently good so that RF leakage is below FCC minimums.[60]

Supplying power to the plasma of an RF-excited transversely pumped CO_2 waveguide laser requires careful design. The RF voltage source typically has a very low impedance, while the laser tube may have an impedance of hundreds to thousands of ohms at its operating frequency. A laser tube with a square bore 4.8 mm in width and 37 cm long, with a laser gas pressure of 60 torr; will have an impedance of approximately 200 ohms when operating with an output of approximately 15 watts.[61] The impedance increases as the power decreases, and is several thousand ohms if the plasma is not ignited.

An impedance matching network typical of the Synrad series 48 lasers is described in U.S. Patent #5,008,894, "Drive System for RF-Excited Gas Lasers," by Peter Laakmann. The basic concept is illustrated in Figure 12.17. An RF power supply output stage is connected through a transmission line to the pair of electrodes and ground strips forming the waveguide laser. The collector of the upper transistor in the push-pull output stage of the RF power supply is connected to the top electrode of the laser through the core of a 1/4 wavelength (at the laser operating frequency) transmission line. The lower transistor in the push-pull output stage is connected through the cladding of the transmission line to ground via a blocking capacitor. A coil connects the top electrode to the bottom electrode of the waveguide laser. (This coil serves to neutralize the capacitive reactance and to generate bi-phase excitation of the plasma.[62]) A transformer is used to match the impedance of the final stage to the preceding circuitry in the RF source.

In a small RF-excited CO_2 laser (such as the Synrad 10-50 watt series 48 lasers) the entire power supply and impedance matching networks can be integrated into a single

---

[60] P. Laakmann, "Using Low Power CO_2 Lasers in Industrial Applications," Synrad Application Note.

[61] P. Laakmann, "Drive System for RF-Excited Gas Lasers," U.S. Patent #5,008,894, April 16, 1991.

[62] P. Laakmann, "Electrically Self-Oscillating RF-Excited Gas Laser," U.S. Patent #4,837,772, June 6, 1989.
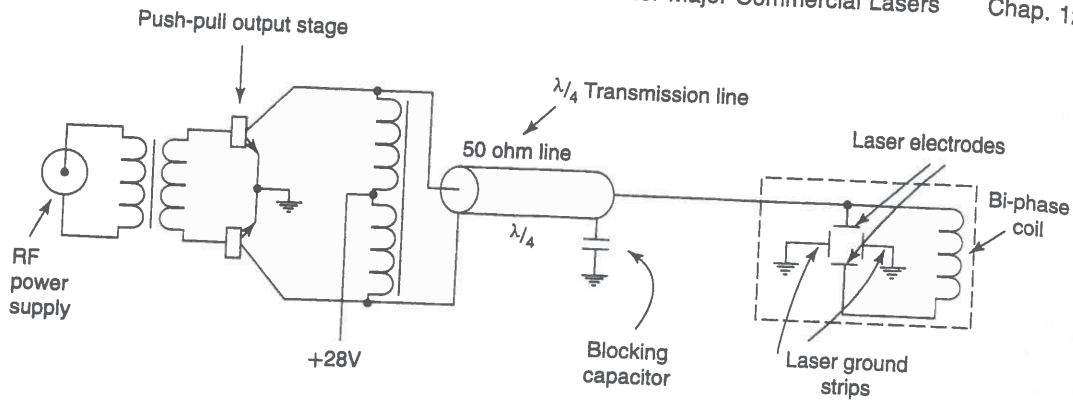
Figure 12.17   An impedance matching network typical of the Synrad series 48 lasers. (From Peter Laakmann, "Drive System for RF-Excited Gas Lasers," U.S. Patent #5,008,894.)
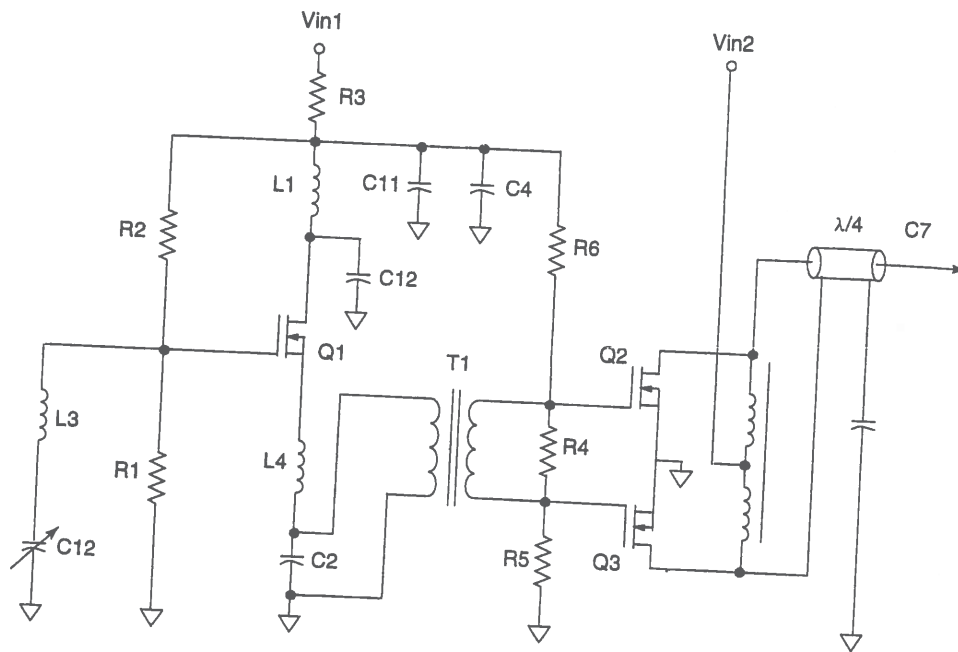
Figure 12.18   A typical RF drive circuit for a waveguide carbon dioxide laser.

unit as illustrated in Figure 12.18. The input stage of the power supply is a relatively conventional RF oscillator circuit. The output stage is a push-pull stage and is integrated into the impedance matching network as described in the previous paragraph and in U.S. Patent #5,008,894.[63]

---

[63]P. Laakmann, "Drive System for RF-Excited Gas Lasers," U.S. Patent #5,008,894, April 16, 1991.

12.1.5 Optical Components and Detectors for CO_2 Lasers

Window, mirrors and lenses.   The long (10.6 μm) wavelength and high average power of CO_2 lasers lead to some difficulties in construction of optical systems. Conventional glass optics cannot be used at CO_2 wavelengths due to high optical absorption and low thermal conductivity. Table 12.1 summarizes the important optical properties of materials typically used for transmissive optics in CO_2 lasers. The alkali halides (such as KBr) tend to have very low absorption, but are hygroscopic and require special coatings to survive in moist environments. The semiconductors (such as ZnSe and GaAs) are much more robust, but with correspondingly higher absorption coefficients. Unfortunately, both germanium (Ge) and silicon (Si) suffer from a thermal runaway problem. Above a certain critical laser intensity, as the sample heats, the absorption increases, and the sample heats more. This feedback mechanism rapidly results in destruction of the sample.

TABLE 12.1   PROPERTIES OF MATERIALS USED IN CO_2 LASERS

Material	Thermal expansion ($\times 10^6$ / °C)	Thermal conductivity ($\times 10^{-2}$ W / cm °C)	α (at 10.6 μm cm^{-1})
NaCl	38.9	6.5	$1.34 \cdot 10^{-3}$
KBr	43	4.8	$5 \cdot 10^{-5}$
ZnSe	7.7	13	$6 \cdot 10^{-3}$
GaAs	5.7	37	$1.2 \cdot 10^{-2}$
Si	4.2	120	2.5
Ge	6	59	$3.6 \cdot 10^{-2}$

W. W. Duley, *CO_2 Lasers: Effects and Applications* (New York: Academic Press, 1976), p. 104, Table 3.4.

Zinc selenide (ZnSe), a well-behaved semiconductor with a relatively high thermal conductivity and low absorption, is the typical choice for CO_2 transmissive optics. ZnSe does not suffer from thermal runaway and has the major advantage of being transmissive from 600 nm to 11 μm. (This allows low power HeNe lasers to be used for alignment of CO_2 systems.) ZnSe is available commercially as in the form of windows, dielectric-coated partially-transmitting mirrors, and lenses.

The very high average power typical of CO_2 lasers means that CO_2 reflecting optics must be thermally conductive as well as poor optical absorbers at 10.6 μm. Dielectric- or metal-coated mirrors with single-crystal silicon substrates are the mirrors of choice for lower-power CO_2 lasers. Higher power lasers use metal coatings (typically silver or gold) on molybdenum or copper substrates. Molybdenum (with a thermal conductivity of 1.33 W/cm °C) offers roughly equivalent thermal conductivity as silicon, but is a much more durable refractory material. Molybdenum may also be used without a surface metal coating of gold or silver. (Uncoated molybdenum mirrors typically have reflectances on the order of 98%.) Copper (with a thermal conductivity of 3.9 W/cm °C) is much more thermally conductive than either silicon or molybdenum, but significantly less rugged. Copper is also difficult to polish and exceptionally easy to scratch during cleaning.

The long wavelength of CO_2 lasers does offer certain advantages during fabrication of optics. Diffraction and focusing effects of scratches are roughly proportional to $(1/\lambda)^4$.

Thus, a relatively poor finish by visible optics standards may be perfectly suitable for CO_2 laser optics. Additionally, the longer wavelength permits fabrication of optics using such methods as diamond turning. If properly fabricated, a diamond turned CO_2 reflector may not need to be polished after fabrication.

CO_2 laser detectors.   The long wavelength and high average power of CO_2 lasers also lead to difficulties in optical detection and laser power measurement. Several detection technologies are commonly employed with CO_2 lasers to overcome these problems. These technologies include thermopiles, bolometers, pyroelectric crystals, and long wavelength semiconductor photovoltaic and photoconductive detectors. (For more details on thermopiles, bolometers, and pyroelectric crystals, see Section 8.4.)

The majority of photovoltaic and photoconductive semiconductor devices are fabricated from silicon and have a roughly 400 nm to 1.1 μm response range. A simple example of a photodetector of this type is a PIN photodiode. However, photovoltaic or photoconductive devices do exist with responses in the 10.6 μm range. To move the detector into the 10.6 μm range requires switching to more exotic semiconductors with narrower bandgaps than silicon. Examples include HgCdTe, CdTe, and PbSnTe. However, 10.6 μm infrared photovoltaic or photoconductive detectors do suffer from a special problem. Semiconductor energy states that absorb in the 10.6 μm range are separated by approximately 0.1 eV. Thus, thermal population of the energy states from sources other than the laser beam is quite likely. Therefore, the detectors are often cooled using liquid helium, liquid nitrogen, or thermoelectric coolers.

10.6 μm radiation is far outside of the human visual response. Thus, a number of techniques have been developed to enable humans to locate the beam and make qualitative measurements. The simplest include such things as absorption in foamed polystyrene, wood, or metal. More complex methods include the use of color changes in liquid crystals and visible fluorescence from various materials. One of the most elegant and effective methods is the thermal-quenching of visible luminescence from a ZnCdS phosphor excited continuously with UV light. The usual configuration is to use a UV light to excite the back of a small screen coated with the phosphor. The phosphor glows a brilliant yellow until it interacts with a CO_2 beam. The CO_2 beam quenches the fluorescence and leaves dark areas on the screen.

12.2 THE DESIGN OF EXCIMER LASERS

Excimer[64] lasers operate on the radiative transition between the excited state of a molecule and its ground state. Commercial excimer lasers typically use molecules formed from the combination of heavy noble gases (such as Xe, Kr, and Ar) and halogens (such as F, Cl, Br, and I). Common excimer laser combinations include ArCl (175 nm), ArF (193 nm), KrCl (222 nm), KrF (249 nm), XeBr (282 nm), XeCl (308 nm), and XeF (351 nm). Excimer lasers operate pulsed and are available in energies ranging from several millijoules to handfuls of

---

[64]In the most correct usage, the word *excimer* is limited to homopolar molecules such as Xe_2. Heteropolar molecules such as XeF are more correctly termed *exciplex* molecules. However, since it is quite difficult to pronounce exciplex laser, the term excimer has grown to mean both classes of lasers.

joules per pulse. Repetition rates range from a few kHz to hundreds of Hz and output average powers are available up to 500 watts.

Excimer lasers are prized for their ability to efficiently produce coherent UV and deep UV radiation. They are used in such diverse commercial applications as laser hole drilling, laser chemical vapor deposition, laser photochemistry, creation of soft x-ray plasmas, semi-conductor wafer cleaning, laser machining, laser ablative sputtering, excimer laser surface annealing, deep UV lithography, and laser planarization. They find application in the medical field for coronary angioplasty and photorefractive keratectomy. Research applications include spectroscopy, laser photochemistry, laser doping of semiconductors, and remote sensing.

Excimer lasers, like CO_2 lasers, are very different from the other lasers discussed in this text. Conventional lasers lase off electronic transitions between various atomic states. Excimer lasers lase off the transition between a molecular excited state and a molecular ground state. This means that excimer lasers tend to have a shorter wavelength and higher efficiency than most conventional lasers. Additional information on excimer lasers can be found in Rhodes,[65] Laude,[66] Elliot,[67] and Weber.[68]

12.2.1 Introduction to Excimer Laser States

Consider a gas mixture of a rare gas A (such a krypton) and 0.1 to 0.3% of a halogen gas X (such as fluorine). Assume that the mixture is pumped by an intense electron beam, which forms A^+ and X^- ions.[69] The ions then recombine to form the excited $(A^+ X^-)^*$ state as:[70]

$$A^+ + X^- + M \rightarrow (A^+ X^-)^* + M \tag{12.4}$$

where A is the rare gas ion, X is the halogen ion and M is any third body (usually another rare gas ion) to assure momentum conservation.

The $(A^+ X^-)^*$ molecules are the excited molecules and form the upper state population (with a lifetime on the order of 5 to 15 ns). The AX molecules form the lower state population. However, the lifetime of the AX molecule is extremely short (on the order of tens of femtoseconds). Thus, even though the upper state lifetime is short by the standard of most lasers (tens of nanoseconds as compared to tens or hundreds of microseconds), it is still three orders of magnitude greater than the lifetime of the ground state. (For excimer lasers to operate correctly, it is necessary for the ground state molecule to dissociate rapidly. Systems for which the molecule dissociates slowly do not make successful lasers because the laser bottlenecks in the ground state.)

---

[65] C. K. Rhodes, ed, *Excimer Lasers* (Berlin: Springer-Verlag, 1984), particularly Chapter 4, pp. 87–138.

[66] Lucien Laude, *Excimer Lasers* (Netherlands: Kluwer Academic Publishers, 1994).

[67] David Elliot, *Ultraviolet Laser Technology and Applications* (San Diego: Academic Press, 1995).

[68] Marvin J. Weber, ed, *Handbook of Laser Science and Technology, Vol. II, Gas Lasers* (Boca Raton, FL: CRC Press, Inc., 1982), particularly Section 3, pp. 273–491; and Marvin J. Weber, ed, *Handbook of Laser Science and Technology, Supp. I, Lasers* (Boca Raton, FL: CRC Press, Inc., 1991), particularly Section 3.3.1, pp. 341–387.

[69] The A^+ and X^- ions are A and X atoms which have lost or gained one electron respectively.

[70] The excited $(A^+ X^-)^*$ is a molecule with the same number of electrons as AX, but with one of the electrons in a higher energy state.
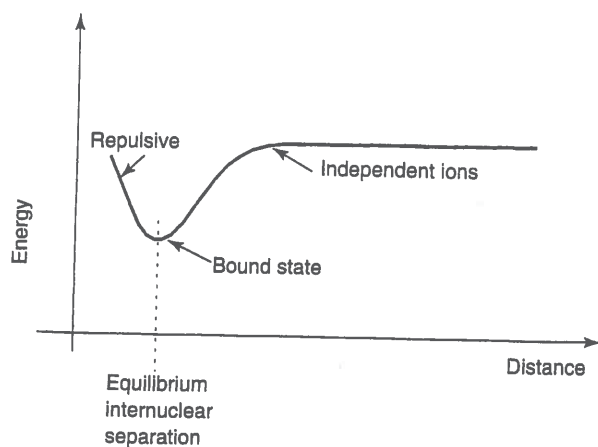
Figure 12.19 The formation of a molecule is driven by a balance between the coulombic attraction of the ions and the repulsive potential that keeps two ions from occupying the same space.

The physics of excimer laser operation is inherently connected to the basic processes of molecule formation. Recall that the formation of a molecule is driven by a balance between the coulombic attraction of the ions and the repulsive potential that keeps two ions from occupying the same space. Thus, the formation of a molecule is a function of the distance between the two ions (see Figure 12.19). If the two ions are widely separated, there is no molecule. If the two ions are trying to occupy the same space, there is no molecule. The balance between the coulombic attraction and the repulsive potential creates a *well* or *pocket* in the potential energy curve. When the two ions are at a distance (the equilibrium internuclear separation) corresponding to this energy well they are *bound* and form the molecule.

The situation in a rare-gas halogen laser is somewhat more complicated than that illustrated in Figure 12.19. This is because of the simultaneous existence of atoms, ions, molecules, and their various excited states. A simplified potential energy diagram of a rare gas halogen excimer laser is illustrated in Figure 12.20. Notice that the upper state manifold has two kinds of potential energy curves. There are covalent curves corresponding to the bonding of an excited atom with another atom ($A^* + X$ or $A + X^*$). There are also ionic curves corresponding to the bonding of two ions (A^+X^-). The ionic curves actually form a family of curves, because there are a variety of electron configurations possible in the $(A^+X^-)^*$ excited state.

Practical excimer laser systems are those for which the ionic $(A^+X^-)^*$ states are the lowest states of the upper manifold. These are systems where the crossings between the ionic and covalent state energies occur for larger internuclear separations than the equilibrium distance. In these systems the dynamics of the reactions lead inevitably to molecules residing in the bound metastable $(A^+X^-)^*$ state. From the $(A^+X^-)^*$ state, the only available downward energy transition is by radiation. There are no competing alternative paths.

The lower state manifold is similar to the upper state manifold, but somewhat less complex. Since the lower state does not have ions, the only potential energy curves are those associated with the various electronic states of the covalent AX. The lower state may (or may not) have a potential well indicating the existence of a bound molecule.

Structure of rare gas monohalides
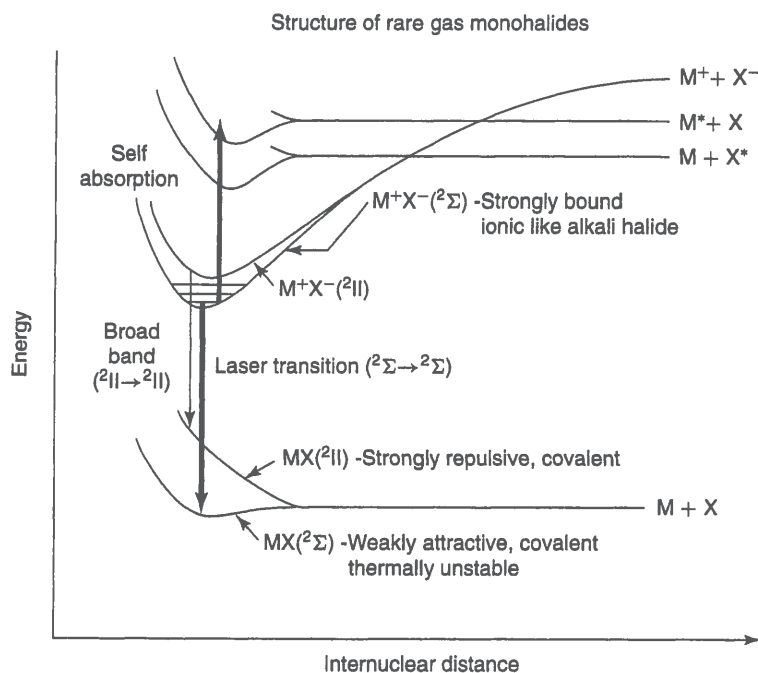
Figure 12.20 A simplified potential energy diagram of a rare-gas halogen laser. (From C. K. Rhodes, ed, *Excimer Lasers* (Berlin: Springer-Verlag, 1984), Figure 4.1, p. 88. ©1984 Springer-Verlag.)

The emission spectrum of KrF illustrates the radiative characteristics of a typical rare gas-halogen transition (see Figure 12.21). The largest peak corresponds to the transition from the bottom of the potential well of the $(A^+X^-)^*$ excited state to the bottom of the potential well of the AX excited state.

Commercially interesting rare gas halide lasers are pumped by electron beam excitation or by electrical discharge. In electron beam excitation, an energetic electron beam is created in vacuum and directed through a thin metal or polymer membrane into the gas mixture. High energy electrons scattering off atoms in the gas create ions, excited atoms, and secondary electrons. The secondary electrons, in turn, create more ions, excited atoms, and electrons. The ions and excited atoms react to form the excited molecules. Under electron beam excitation, ions are produced in preference to excited states (by about a 3:1 ratio) and the primary reaction is
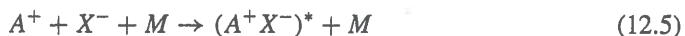
$$A^+ + X^- + M \rightarrow (A^+X^-)^* + M \qquad (12.5)$$

where A is the rare gas ion, X is the halogen ion, and M is any third body (usually another rare gas ion), to assure momentum conservation.

Pulsed electrical discharges are more commonly used for commercial lasers because they offer the potential for higher pumping efficiency and higher average power. In an electrical discharge, the low energy electrons drift along in the electric field and increase in energy. Eventually, they reach the energy threshold for excitation of the first excited state
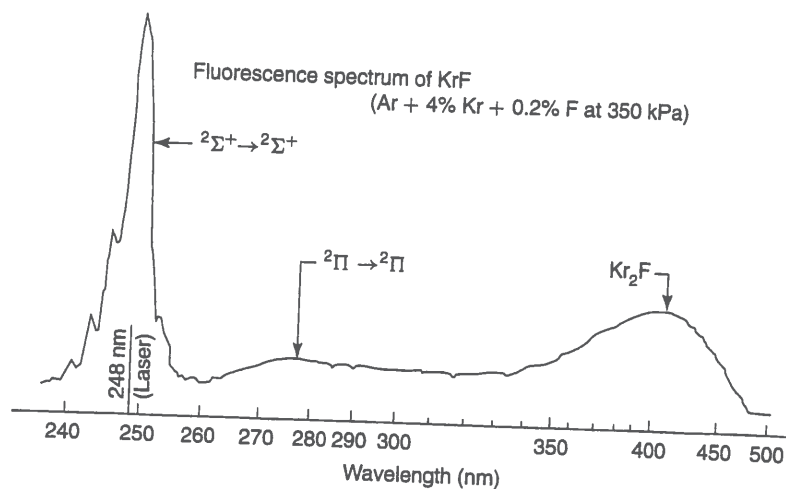
Figure 12.21 The emission spectrum of KrF illustrates the radiative characteristics of a typical rare gas-halogen transition. (From C. K. Rhodes, ed, *Excimer Lasers* (Berlin: Springer-Verlag, 1984), Figure 4.2, p. 91. ©1984 Springer-Verlag.)

of the rare gas atoms. Then, they collide inelastically with the rare gas atom, leaving the gas atom in an excited state and returning the electron to low energy. Under these conditions, a very fast and efficient reaction termed a *harpoon* collision is involved.[71]

$$A^* + MX \rightarrow (A^+X^-)^* + M \tag{12.6}$$

12.2.2 The Evolution of Excimers

The first excimer was demonstrated in 1970 by Basov et al. at the Lebedev Physics Institute.[72] This laser was an Xe_2 excimer that lased at 176 nm and was excited by a relativistic electron beam directed into liquid xenon. In 1972, Koehler et al. at Lawrence Livermore National Laboratories demonstrated an Xe_2 laser using electron beam pumping of gaseous xenon.[73] Laser action from XeBr at 282 nm was first reported in 1975 by Searles and Hart at the Navel Research Laboratory.[74] Searles and Hart measured the optical gain of the XeBr to be 4% per pass over 15 cm of active length. The experiment was originally run at 1 to 4% Br_2, but this was reduced to 0.1 to 1% Br_2 when the Br_2 was discovered to quench the XeBr excited state.

A few weeks later, Ewing and Brau reported laser action from XeCl at 308 nm and KrF at 249 nm.[75] An independent observation of laser action in KrF was also reported by Tisone

[71]D. R. Herschbach, *Adv. Chem. Phys.* 10:319 (1966); pp. 367–379 in particular.

[72]N. G. Basov, V. A. Danilychev, Yu. M. Popov, and D. D. Khodkevich, *JETP Lett.* 12:329 (1970).

[73]H. A. Koehler, M. A. Ferderber, D. L. Redhead, and P. J. Ebert, *Appl. Phys. Lett.* 21:198 (1972).

[74]S. K. Searles and G. A. Hart, *Appl. Phys. Lett.* 27:243 (1975).

[75]J. J. Ewing and C. A. Brau, *Appl. Phys. Lett.* 27:350 (1975).

et al.[76] and Mangano and Jacob.[77] In the Ewing and Brau experiments, laser action was obtained from a mixture of Ar, Xe, and Cl_2 at 89.9:10:0.1 and from a mixture of Ar, Kr, and F_2 at 98.9:1.0:0.1. The output energy was approximately 50 μJ from the XeCl laser and approximately 4 mJ from the KrF laser. Tisone et al. used a mixture of 3000 torr of Ar, 150 torr of Kr, and 6 torr of F_2 and were able to obtain 5.6 J by using 5 cm diameter cavity mirrors. In the Mangano and Jacob experiments, laser action was obtained from a mixture of Ar, Kr, and F_2 at 97.9:2.0:0.1. The maximum output energy in the Mangano and Jacob experiments was 6 mJ. All three experiments used a pulsed electron gun to excite the gas mixture.

Reports of laser action from XeF soon followed, first discovered by Brau and Ewing,[78] but first published by Ault et al.[79] Brau and Ewing used a mixture of Ar, Xe, and F_2 at 99.6:0.3:0.1 where the mixture was excited with a cold cathode electron gun. Ault et al. used a mixture of Ar, Xe, and NF_3 at 250:25:1. The use of NF_3 in the Ault experiments was to both minimize the corrosive effects of F_2 and to avoid quenching due to self-absorption. The measured output energy from the Ault experiments was 5 mJ per pulse, the peak power was 500 kW, and the pulse width was 10 ns.

All of the early excimer and exciplex lasers were electron beam pumped. However, the efficiency advantages of using electrical discharge pumping were recognized very early. Since excimer lasers require very high voltages, longitudinal discharge excitation of excimers was never successfully attempted. Instead, excimer technology leveraged off the existing developments in transversely excited CO_2 lasers. A major advancement occurred in 1975, when Burnham and Djeu at the Navel research laboratories modified a TEA CO_2 laser and demonstrated excimer laser action with an electrical discharge.[80]

12.2.3 General Design Background

Gas flow. In order to operate an electrically discharge excited excimer laser, it is necessary to provide an electric field that exceeds the DC breakdown voltage of the gas mixture by a factor of 2 to 3. This typically requires voltages of 10 to 15 kV/cm. Furthermore, this pulse must be applied in a time short compared to the electronic avalanche time of 20 to 30 ns. This implies a rise time of several kV/nanosecond. Finally, there must be sufficient electrons in the circuit to supply the growing plasma. This requires a very low impedance electrical excitation circuit.

The discharge pulse of an excimer laser creates a number of ionized and excited species. Many of these species are quite long-lived. If another discharge pulse is attempted before these secondary species have decayed, the resulting electrical discharge will be unstable. Therefore, in most commercial excimers, the gas flows across the electrodes. In general, the best results are achieved when the flow rate is high enough to flush the dis-

---

[76]G. C. Tisone, A. K. Hays, and J. M. Hoffman, *Opt. Commun.* 15:188 (1975). (The Ewing paper was received on June 17, 1975, and the Tisone paper on July 7, 1975.)

[77]J. A. Mangano and J. H. Jacob, *Appl. Phys. Lett.* 27:495 (1975). (The Ewing paper (footnote #75) was received on June 17, 1975, and the Mangano paper on July 7, 1975.)

[78]J. J. Ewing and C. A. Brau, *Appl. Phys. Lett.* 27:350 (1975); and C. A. Brau and J. J. Ewing, *Appl. Phys. Lett.* 27:435 (1975).

[79]E. R. Ault, R. S. Bradford, and M. L. Bhaumik, *Appl. Phys. Lett.* 27:413 (1975).

[80]Jeff Hecht, *Laser Pioneers*, revised ed. (Boston, MA: Academic Press, 1992), p. 46.

charge volume between the electrodes 2 to 3 times before the next pulse. In the case of high power lasers with pulse repetition rates of 500 Hz to 2 kHz, this gas replacement means that velocities of 50 to 150 m/sec are required. Thus, aerodynamics becomes a critical part of excimer laser design.

Preionization.

Good electrical discharge uniformity is essential for the successful operation of a pulsed excimer laser. In order to provide a uniform high voltage discharge in high pressure gases, the gas must be preionized immediately prior to the application of the main electrical discharge pulse. Preionization means that a uniform ion or electron cloud is generated in the gas in the discharge region. This cloud serves to *seed* the discharge and prevent the formation of arcs or streamers in the discharge. Once the initial cloud (approximately 10^7 electrons/cm^3) is created, the main discharge will proceed by avalanche ionization to create densities near 10^{15} electrons/cm^3.

Preionization is a very challenging problem because a large number of electrons must be created quickly. Preionization can be accomplished in a variety of ways.[81,82] The two most common are UV light and x-rays. UV light can be generated by spark gaps or by corona discharges. However, UV light does have the limitation that the ionizing range is restricted to a few cm.[83] X-rays can be created in x-ray tubes by collisions of energetic electrons with a high Z material (such as tungsten). X-rays have a much deeper penetration depth, but are more difficult to create. In addition, the use of x-rays in a commercial system requires special licensing and approval.

Multiple spark gaps are commonly used to create UV light for preionization.[84] Early excimer laser systems used a linear sparkboard where each spark gap was separately discharged to create a traveling spark wave down the length of the cavity. Later designs used multiple parallel pins, where the pins were fired simultaneously. Spark gaps provide excellent preionization, but at the cost of some structural complexity. More importantly, spark gaps erode and tend to contaminate the laser gas and optical components of the resonator. Spark gaps are much less frequently used today, as they have been replaced by corona or x-ray preionization methods.

Corona discharges tend to provide lower electron concentrations, but are structurally simpler and do not contaminate the gas. Corona discharges have the additional advantage that they can be easily integrated with the main electrode structure. Thus corona discharges are most commonly used with commercial excimers (such as XeCl) that do not require high electron preionization concentrations.

Another alternative is to use x-ray preionization.[85] Although x-ray preionization was not used in the early development of excimer lasers (due to the difficulty and expense of making short x-ray pulses) advances in x-ray generation technology for lasers have made x-ray preionization a very viable alternative to corona technology. This is especially true for the more exotic excimers which may require higher preionization electron densities.

[81] A. J. Palmer, *Appl. Phys. Lett.* 25:136 (1974).

[82] S. C. Lin, *J. Appl. Phys.* 51:210 (1980).

[83] K. Midorikawa, M. Obara, and T. Fujiokam, *IEEE J. of Quantum Electron.* QE-20:198 (1984).

[84] K. Miyazaki et al., *Rev. Sci. Instrum.* 52:201 (1985).

[85] S. Sumida, M. Obara, and T. Fujiokam, *Appl. Phys. Lett.* 33:913 (1978).
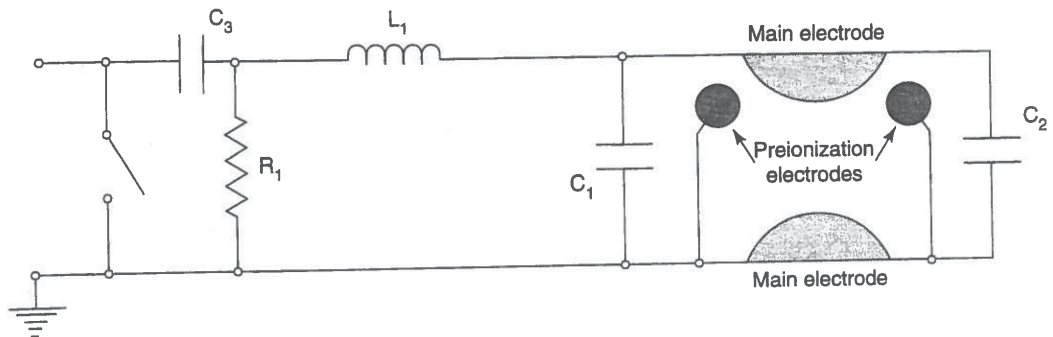
Figure 12.22 A typical corona discharge circuit. The two main electrodes are oriented transversely. The two preionization electrodes are also oriented transversely, and are parallel to the main electrodes. (From E. Müller-Horsche, "Apparatus for Preionizing a Pulsed Gas Laser," U.S. Patent #5,247,531, Sept. 21, 1993.)

Corona discharge circuitry.   The corona discharge method is one of the most common commercial preionization techniques.[86,87] In the corona discharge method, UV light is generated by a gas discharge between a metal and a dielectric. The UV light then creates a weak ionization in the discharge region of the electrodes. One of the major advantages of corona preionization is that the dielectric prevents formation of spark channels to the preionization electrodes. Thus, the contamination effects of the sparks are eliminated.

A typical corona discharge circuit is shown in Figure 12.22.[88] The two main electrodes are oriented transversely. The two preionization electrodes are also oriented transversely, and parallel to the main electrodes. The preionization electrodes consist of a conductor with a surrounding dielectric (for example, a quartz sleeve). The preionization electrodes are placed near one of the main electrodes and are connected to the potential of the other electrode. A high-voltage source charges the storage capacitor, and the pulse is triggered by a thyratron (or equivalent high-voltage switching element). The preionization potential is thus driven by the main discharge pulse.

Another option is shown in Figure 12.23.[89] The geometry is similar to Figure 12.22. However, with this system, the preionization potential is driven by a separate set of circuitry from the main discharge pulse. This permits more subtle tuning of the timing between the two events, but at the cost of additional circuitry.

Still another option is shown in Figure 12.24.[90] Here, the clever use of inductors and capacitors generates a very rapid starting spike across the preionization electrodes, which is followed by the main discharge pulse. Suitable choice of inductor and capacitor values permit this circuit to be tuned for optimum output power.

---

[86]G. J. Ernst and A. G. Boer, *Opt. Commun.* 27:105 (1978).

[87]U. Hasson and H. M. Bergmann, *Rev. Sci. Instrum.* 50:59 (1979).

[88]E. Müller-Horsche, "Apparatus for Preionizing a Pulsed Gas Laser," U.S. Patent #5,247,531, Sept. 21, 1993.

[89]E. Müller-Horsche, "Apparatus for Preionizing a Pulsed Gas Laser," U.S. Patent #5,247,531, Sept. 21, 1993.

[90]E. Müller-Horsche, "Apparatus for Preionizing a Pulsed Gas Laser," U.S. Patent #5,247,531, Sept. 21, 1993.
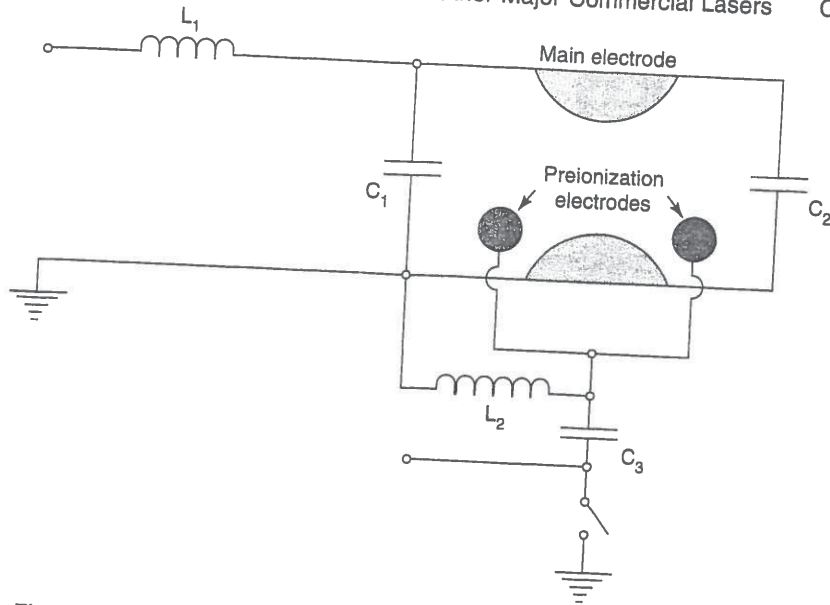
Figure 12.23   Another type of corona discharge circuit. In this circuit, the preionization potential is driven by a separate set of circuitry from the main discharge pulse. This permits more subtle tuning of the timing between the two events, but at the cost of additional circuitry. (From E. Müller-Horsche, "Apparatus for Preionizing a Pulsed Gas Laser," U.S. Patent #5,247,531, Sept. 21, 1993.)
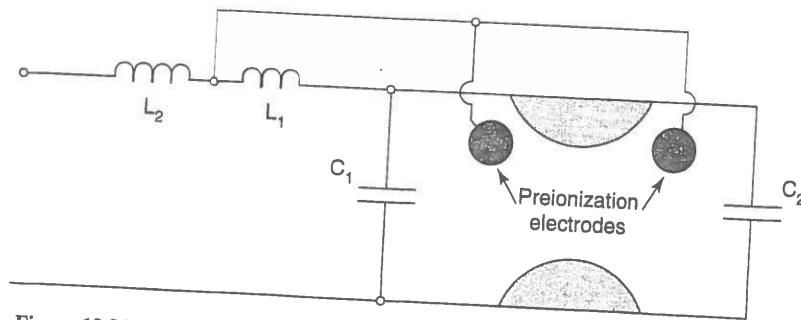
Figure 12.24   In this circuit, the clever use of inductors and capacitors generates a very rapid starting spike across the preionization electrodes, which is followed by the main discharge pulse. (From E. Müller-Horsche, "Apparatus for Preionizing a Pulsed Gas Laser," U.S. Patent #5,247,531, Sept. 21, 1993.)

Main discharge circuitry.   Once the preionization stage is complete, the main discharge pulse must be generated. The electrical discharge requirements on discharge excited pulsed excimer lasers are quite stringent. The rise time is short (10^{11} A/sec) and the voltage and power are high (50 kV and 5 kW). Furthermore, the gas (after breakdown) has a very low impedance.
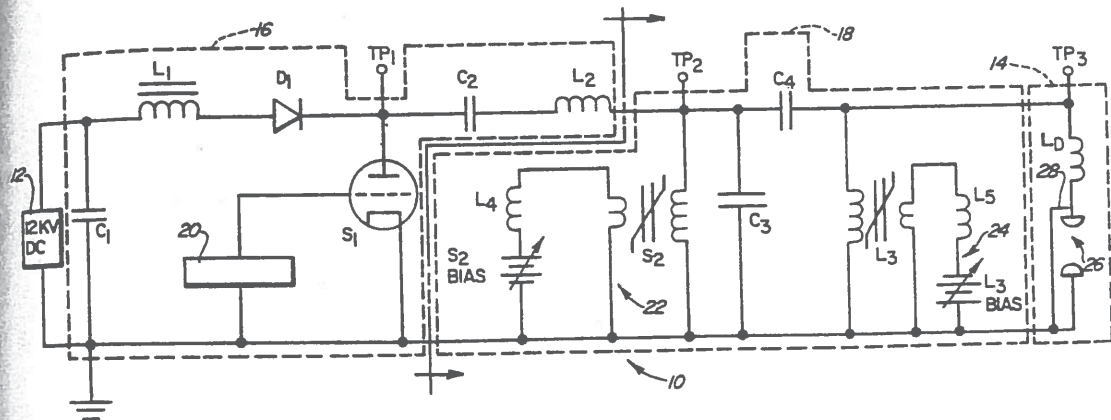
Figure 12.25 A typical discharge circuit for an excimer laser. This circuit provides an electrical interface between a high-voltage, high-impedance power source, and a relatively low-impedance laser load. (From T. S. Fahlen and B. Mass, "Electrical Excitation Circuit for Gas Lasers," U.S. Patent #4,549,091, Oct. 22, 1985.)

An example of a typical discharge circuit is shown in Figure 12.25.[91] The electrical circuit provides an electrical interface between a high-voltage, high-impedance power source and a relatively low-impedance laser load. The circuit includes an electrical excitation circuit 10, a charging circuit 16, a pulse forming network 18, and a laser load 14.

The charging circuit includes a power source capacitor C_1, a charging capacitor C_2 series-connected with an inductor L_2, a charging choke L_1 and an isolating diode D_1. The choke L_1 and charging diode D_1 isolate the power source 12 from the pulse forming network 18. (The capacitor C_1 is significantly larger than the capacitor C_2.) A thyratron S_1 is also included in the charging circuit. The control electrode of the thyratron is connected to a pulse generator.

The pulse-forming network (PFN) includes a saturable inductor switch S_2, a bias power source for S_2, and a choke L_4 connected in series with the bias winding of the saturable inductor switch. The PFN also includes a PFN capacitor C_3 shunted across the saturable inductor switch S_2 and a second PFN capacitor C_4 connected between TP_2 and TP_3. Additionally, the PFN includes a magnetic diode charging inductor L_3, a bias power source for L_3 and a choke L_5 connected in series with the bias winding of the magnetic diode charging inductor. (The choke L_5 provides isolation of the bias power source for L_3 from high-voltage pulses produced by transformer action on the bias winding of the magnetic diode-charging inductor L_3.) The laser load 14 is connected between TP_3 and common. The inductance L_D represents the distributed inductance of the electrode structure of the laser load 14. A preionization circuit 28 is also included.

The electrical excitation circuit performs four relatively separate operations: a slow resonant charge of the charging capacitor C_2, a medium-speed charge of the pulse forming

---

[91] T. S. Fahlen and B. Mass, "Electrical Excitation Circuit for Gas Lasers," U.S. Patent #4,549,091, Oct. 22, 1985.

Electrodes

Preionizer

PFN circut

Inner
dielectric
cylinder

Blower
fans

Heat
exchanger

Outer metal
cylinder
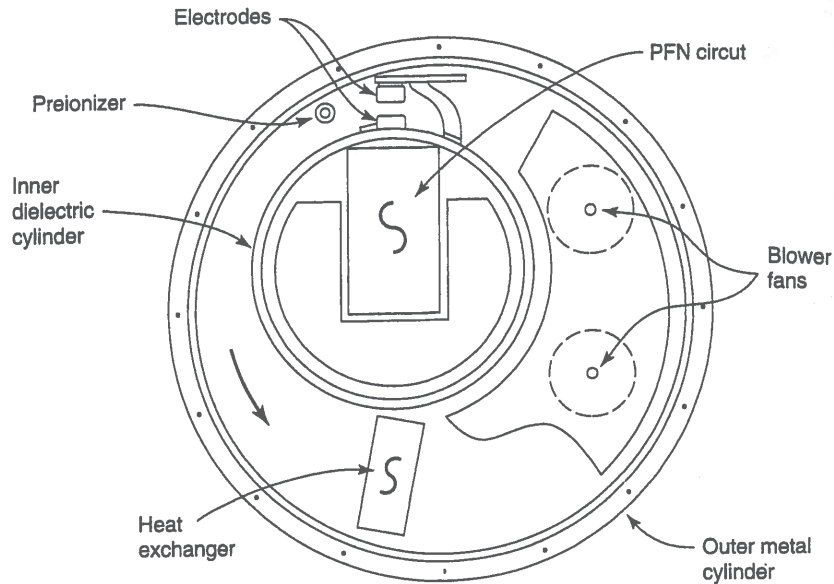
Figure 12.26 The heart of the 5300 is a pressure vessel consisting of two eccentrically mounted cylinders. (From D. J. Clark and T. S. Fahlen, "Gas Transport Laser System," U.S. Patent #4,611,327, Sept. 9, 1986.)

network 18, an inversion of the voltage on half of the pulse forming network, and finally the laser discharge.

12.2.4 A Typical Modern Excimer Laser

The remainder of this section will focus on an industrial excimer laser intended for industrial materials processing applications. The specific unit under discussion is the XMR 5300 laser manufactured by XMR, Inc., in Fremont, CA. This laser is representative of a high-end industrial materials processing excimer laser.

The XMR 5300 is a XeCl laser operating at 308 nm and producing 200 watts at 300 Hz for an energy of approximately 660 mJ/pulse. The repetition rate is selectable from 1 to 300 Hz and the pulse width is 40 to 50 ns. The output beam incorporates a beam homogenizer and is 1.5 cm by 3.3 cm with less than a 5 mrad divergence. The laser operates at a pressure of 5.76 atmospheres with a buffer gas of neon and uses an HCl precursor to generate the chlorine. The design of this laser is discussed in D. J. Clark and T. S. Fahlen, "Gas Transport Laser System," (U.S. Patent #4,611,327), and in T. S. Fahlen, "Gas Discharge Laser Having a Buffer Gas of Neon," (U.S. Patent #4,393,505), and is only summarized here.[92,93]

The heart of the 5300 is a pressure vessel consisting of two eccentrically mounted cylinders (see Figure 12.26). The outer cylinder is metal and constitutes the outer wall of the pressure vessel. The inner cylinder is a dielectric and contains the PFN for the electrodes.

[92] D. J. Clark and T. S. Fahlen, "Gas Transport Laser System," U.S. Patent #4,611,327, Sept. 9, 1986.

[93] T. S. Fahlen, "Gas Discharge Laser Having a Buffer Gas of Neon," U.S. Patent #4,393,505, July 12, 1983.

The gas flow is between the inner cylinder and the outer cylinder and is driven by a set of blower fans. A gas-to-liquid heat exchanger is located near the bottom of the pressure vessel.

The electrodes are placed on the top of the inner dielectric cylinder and the laser is excited transversely. Two pairs of preionizing corona electrodes are located slightly to both sides of the main electrodes. The main discharge plasma is created between the two electrodes near the top of the pressure vessel. Thus, the optical cavity is located parallel to these electrodes.

Physically, the 5300 pressure vessel consists of a nickel-plated stainless-steel cylinder that is 100 cm long and 60 cm in diameter. The vessel contains approximately 200 liters of laser gas. The stainless-steel cylinder has a welded flange with an o-ring groove on each end. End plates are bolted to the welded flanges. Although the system operates at a pressure of roughly 70 psig, the heavy stainless construction has been pressure tested up to 180 psig.

The laser system is designed for easy repair and maintenance. All of the components inside the pressurized vessel are readily accessible. A removable cantilevered arm hinged to the flange holds the end plate so that it can be swung away from the flange. Once removed, the end plate is supported on a wheeled cradle. The inner dielectric cylinder, electrodes, PFN, blowers, and heat exchangers are attached to the end plate and are removed with it. This configuration provides ready access to the sub-assemblies for servicing. Each of the sub-assemblies is a module and can be replaced independently of the others.

The electrodes are two solid-rail electrodes, 79 cm long and 2.5 cm wide, spaced by 2.5 cm. The material of both electrodes is solid nickel. The electrodes are mounted to the outside of the internal dielectric cylinder. Each of the electrodes is bolted to eighteen feedthroughs penetrating the inner dielectric cylinder. Each feedthrough is o-ring-sealed as it enters the inner cylinder. However, the electrodes can be adjusted or removed without replacing the o-rings.

Five to 10 kW of heat is generated in the laser gas from the electrical discharge, the corona preionization, and the blower fans. The gas to liquid heat exchanger maintains the gas temperature at 90°F with a 65°F input coolant temperature at a flow of 3 to 5 gallons per minute. The heat exchanger is a finned tube construction, nickel-plated to minimize damage from the gas mixture. In order to minimize feedthroughs, the heat exchanger is welded to a flange, which is sealed to the end plate with an o-ring.

Figure 12.27 is a perspective figure illustrating the entire system. The outer metal cylinder defines the shape of the entire system. The inner dielectric cylinder can be seen toward the back of the drawing (somewhat hidden by the fans). The window for the optical cavity can be seen near the front top of the pressure vessel. The large triangular housings on each side of the pressure vessel contain the drive assembly for the blower fans.

The double cylinder structure offers a number of advantages. To begin with, it places the pulse-forming network inside of a large steel structure. This serves as an ideal *Faraday cage* and minimizes the laser generating damaging electromagnetic interference from the extremely high voltage and current pulses. The Faraday cage construction similarly reduces the possibility of accident triggering of the PFN by external sources. Locating the PFN close to the electrodes minimizes the overall inductance of the electrical system. Finally, locating the PFN within the pressure vessel minimizes the number of feedthroughs.
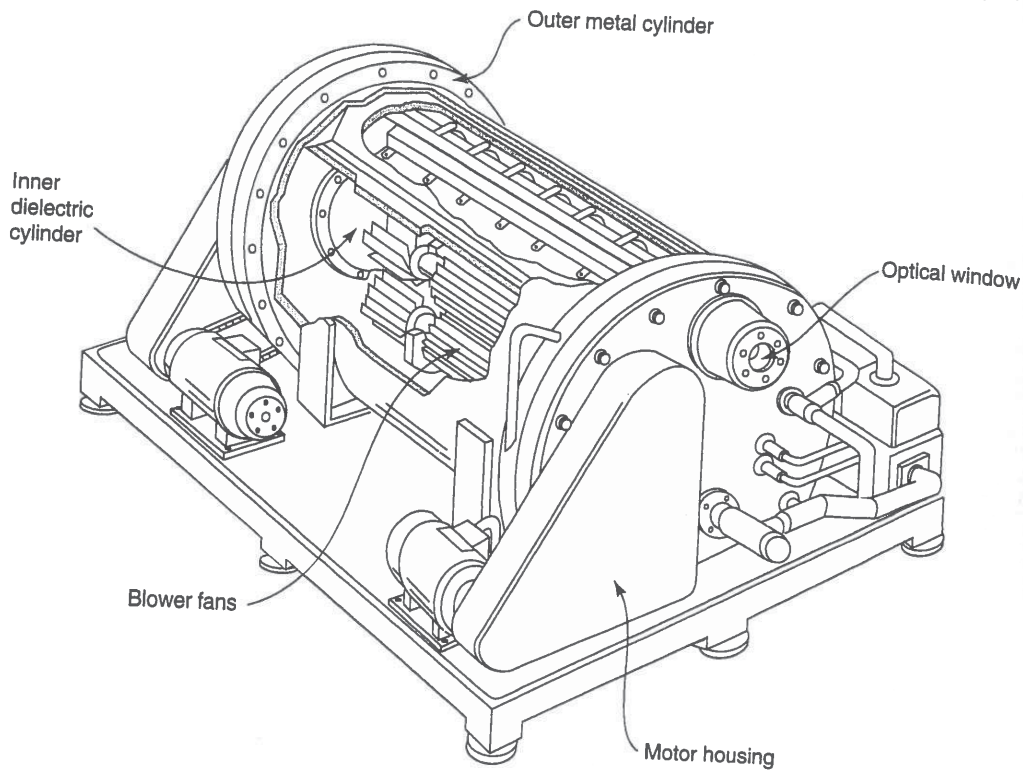
Figure 12.27 A perspective figure illustrating the laser chamber of the XMR 5300. The outer metal cylinder defines the shape of the entire system. The inner dielectric cylinder can be seen toward the back of the drawing (somewhat hidden by the fans). (From D. J. Clark and T. S. Fahlen, "Gas Transport Laser System," U.S. Patent #4,611,327, Sept. 9, 1986.)

The eccentric placement of the cylinders is also a critical part of the design. Notice that the electrodes are located at the narrowest part of the structure. This increases the velocity of the gas over the electrodes and enhances the uniformity of the gas flow. The flow velocity is maximized in the double-cylinder geometry because there are no sharp bends, constrictions, or changes in direction. Additionally, the cylindrical geometry minimizes the surface area exposed to the gas mixture.

One of the major challenges in constructing excimer laser systems is the corrosion caused by the halogen ions. Early excimers were notorious for blowing seals and destroying electrical components. Thus, excimer laser design must include a number of features to simultaneously reduce leakage and enhance the laser lifetime. The 5300 incorporates magnetic couplings for the blowers in order to provide a hermetic seal with no mechanical contact. Within the pressurized vessel, bearings are lubricated with fluorinated lubricants. The blower and coupling bearings inside the vessel are enclosed in a housing, which is pressurized with a small flow of halogen-free gas. In addition, materials used inside the pressure vessel have been selected carefully. The majority of the metals are nickel-plated. Insulating materials are quartz or ceramic.

Viewing Angle

Figure 12.28 Materials processing applications (such as laser planarization or laser annealing) frequently require a "top hat" beam profile with adjustable x and y dimensions. (Courtesy of XMR, Fremont, CA)

The pressure vessel has an input and exhaust port for gas replenishment. Although the 5300 can run for approximately 10^7 pulses without replenishment, eventually parasitic chemical reactions will deplete the halogen and the system will need to be recharged.

The preionization is supplied by a corona wire. The corona wire is a quartz insulated conductor. The discharge volume created by the corona wire is approximately $70 \times 2.5 \times 2$ cm^3.

It is usually necessary to provide a buffer gas in an excimer laser mixture in order to initially support the discharge. Many excimers use helium, because it is chemically inert, inexpensive, has a high ionization potential, and forms stable low pressure discharges. It is also light and has a high specific heat for cooling. However, the 5300 uses neon as a buffer gas. Neon offers many advantages over helium in a system with corona wire preionization. Use of neon as a buffer gas increases both the output power and efficiency of the laser. This enhanced performance appears to be related to increased stability of the plasma.

The electrodes are pulsed at 20 to 50 kV. The rise time of the electrical pulse must be shorter than the upper state lifetime (5 to 15 ns). All of the circuit elements in the PFN are preferably insulated by a bath of transformer oil. The insulating oil is cooled by circulation through a heat exchanger. Electrical connections from the pulse forming network to the external circuitry are made with continuous cables sealed by compression o-rings.

The laser resonator uses a conventional high-reflecting rear mirror and partially transparent front mirror. The laser runs in a pseudowaveguide mode in the vertical direction and in a free-space mode in the horizontal. This creates a beam profile that is Gaussian only in the horizontal direction.

12.2.5 Laser Beam Homogenizers
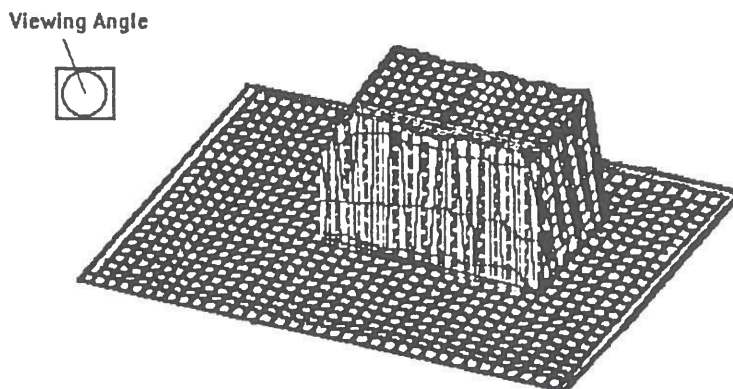
Materials processing applications (such as laser planarization or laser annealing) frequently require a "top hat" beam profile (see Figure 12.28) with adjustable x and y dimensions.

Since most materials processing lasers lase on some combination of Gaussian modes, an optical element (called a homogenizer) is necessary to convert the Gaussian beam into the "top hat" profile. A large number of techniques have been used to homogenize laser beams. One class of techniques consists of using lenses, white cells, or waveguides to divide the beam into small parts and then recombine the parts into the desired shape.[94,95] A second class of techniques uses prisms or mirrors to fold the beam onto itself.[96]

XMR uses a homogenizer of the beam dividing type. In their homogenizer,[97] two sets of arrays of crossed cylindrical lenses (four groups of cylindrical lenses in total) are used to divide the incoming beam into an array of "beamlets" (see Figure 12.29). A focusing lens then recombines the beamlets into a "top hat" distribution on the exposure plane. In the XMR commercial unit, arrays 3 and 4 (and the focusing lens) are fixed. Arrays 1 and 2 are free to move. The separation of array 1 from array 3 determines the x dimension of the homogenized beam, while the separation of array 2 from array 4 determines the y dimension. Notice that the homogenized "top hat" distribution is always formed at the same location from the homogenizer, independent of the location of the arrays.

12.2.6 Application Highlight

Excimer lasers are employed in a large number of laser materials processing applications. The short wavelength, high energy, and high average power of excimer lasers present unique materials processing benefits.

For example, the polysilicon thin film transistor (poly-Si TFT) is considered to be the next technological step in the development of active-matrix liquid crystal displays.[98] Polysilicon has a number of advantages over amorphous silicon. As one example, polysilicon possesses more than 100 times the carrier mobility of amorphous silicon, thus enabling CMOS peripheral display drivers to be integrated right into the display. Displays with built-in drivers are more reliable than conventional displays, because electrical connections are implemented in metallization layers on the substrate itself instead of with thousands of TAB-bonded interconnects. Another benefit of eliminating TAB-bonding is that screen pitch is no longer limited by interconnection pitch, thus opening the door to super-high-resolution displays suitable for imaging and graphics applications. In addition, high mobility poly-Si TFT transistors offer fast charging speeds to compensate for RC time delays in larger displays.

However, commercializing the use of poly-Si TFT devices for active-matrix liquid-crystal displays has been difficult. The customary approach to creating poly-Si TFT devices is to use a quartz substrate with a layer of deposited amorphous silicon and slowly anneal (700°C for 24 hours) the amorphous silicon into a polysilicon thin film. However, the high cost of quartz substrates and the long process times required for furnace annealing have made

---

[94]Geary, *Optical Engineering* 27:972 (1988).

[95]Iwasaki et al., *Applied Optics* 29:1736 (1990).

[96]Bruno and Liu, *Lasers and Applications* (1987), p. 91.

[97]T. S. Fahlen, S. B. Hutchison, and T. McNulty, "Optical Beam Integration System," U.S. Patent #4,733,944, March 29, 1988.

[98]D. Zankowsky, *Laser Focus World* (1994).
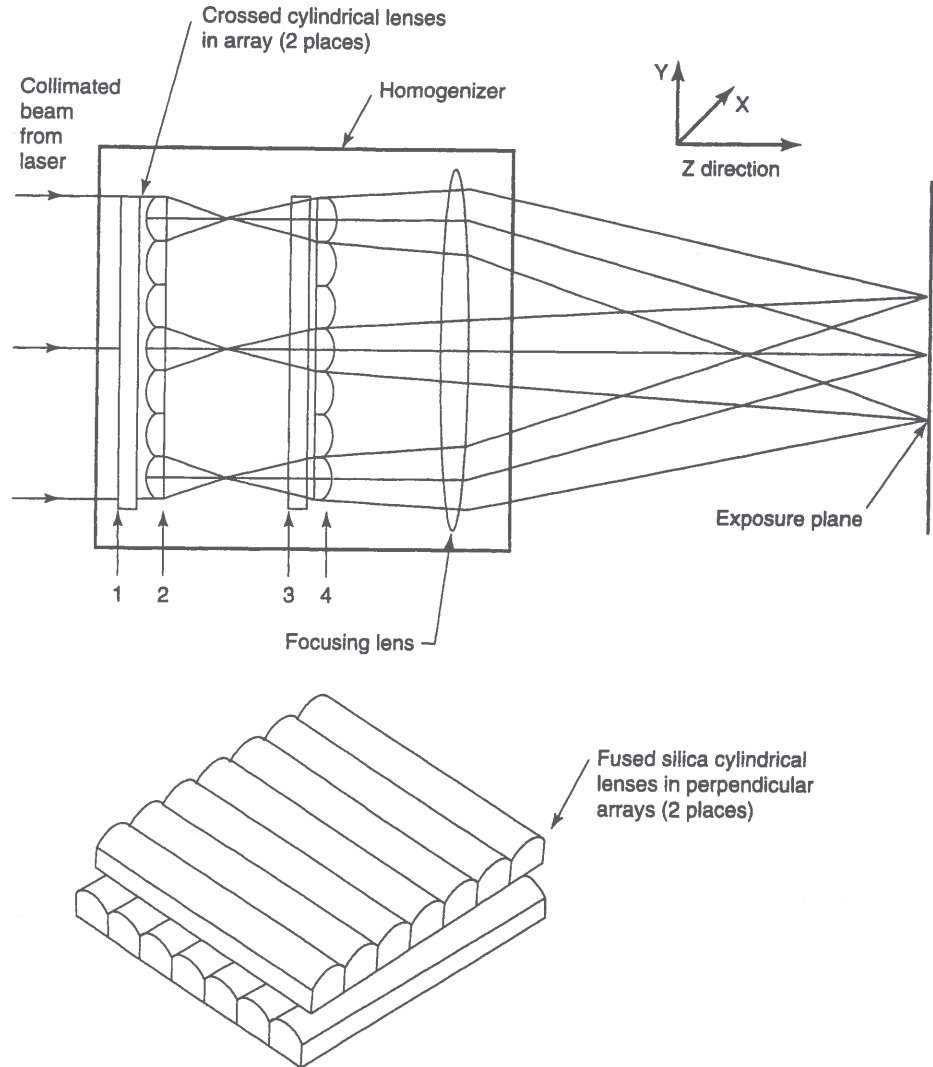
Figure 12.29   In XMR's homogenizer, two arrays of crossed cylindrical lenses (four groups of cylindrical lenses in total) are used to divide the incoming beam into an array of "beamlets." A focusing lens then recombines the beamlets into a "top hat" distribution on the exposure plane. (Courtesy of XMR, Fremont, CA)

this process impractical for high-volume production of large displays. Unfortunately, lower-priced glass substrates cannot be used, because the high temperatures used in conventional annealing processes also melt the glass substrate.

Laser annealing offers an alternative to furnace annealing for creating economical poly-Si TFT devices (see Figure 12.30). In laser annealing, the laser only heats the surface of the material, thus allowing materials other than expensive quartz to be used as substrates.
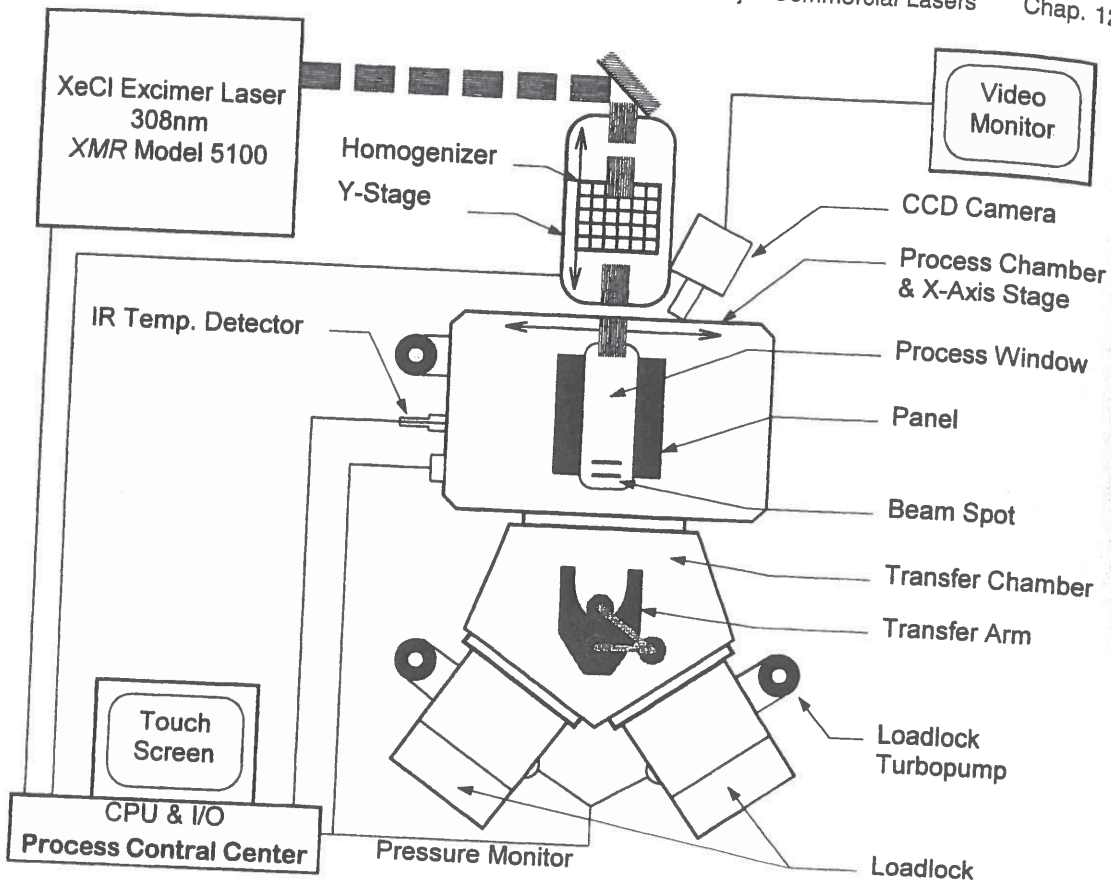
Figure 12.30 Schematic of an excimer laser annealing system for manufacturing poly-Si TFT devices. (Courtesy of XMR, Fremont, CA)

Both argon and excimer lasers have been used to anneal amorphous silicon to polysilicon. However, excimer lasers have a significant advantage over argon lasers in this application. This is because excimers are high power (200+ watt), short pulse (20- to 50-ns) lasers. As a consequence, they only locally heat the surface of the film. The melt region extends just 50 to 100 nm below the surface. Excimer laser annealing is the only current annealing technology that can reliably transform amorphous silicon into polysilicon while the substrate remains at room temperature.

The basic process for creating polysilicon thin films by laser annealing is quite straightforward. Before processing, the substrate is covered with an amorphous silicon thin film. The excimer then scans the glass substrate with a spatially uniform pattern of overlapping rectangular pulses. The UV energy is strongly absorbed by the surface layer of amorphous silicon, which rapidly melts and recrystallizes into polysilicon. The instantaneous local temperature in the surface layer is high enough to achieve excellent crystallinity. However, the

average temperature of the glass substrate remains substantially below the damage threshold and is unaffected by the laser crystallization process.

Since laser annealing is a scanning process, it offers considerable present and future process flexibility. The manufacturer has the option of selectively annealing designated areas or moving to larger or smaller substrates. In addition, laser annealing provides the high throughputs required for high-volume active-matrix liquid crystal display manufacturing. The high peak energy of the excimer laser, combined with a 300 Hz pulse repetition rate, enables 360 × 450 mm substrates to be processed in as little as three minutes.

12.3 OVERVIEW OF SEMICONDUCTOR DIODE LASERS

12.3.1 History of Semiconductor Diode Lasers

There are often periods in science when major discoveries are made simultaneously by a number of different researchers. The early history of semiconductor diode lasers follows this pattern.

Consider the research environment for lasers in mid-1962. The existing lasers were lasers with long path lengths and large external resonators. These lasers lased on narrow transitions between well-defined discrete states. Semiconductors (with a high free carrier absorption, wide bandwidth optical transition, and relatively small size) were assumed to have inefficient radiative recombination and were considered an improbable material for laser action.

However, in July 1962 Keyes and Quist presented a paper, "Recombination Radiation Emitted by Gallium Arsenide Diodes," at the Solid State Device Research Conference (SSDRC) in Durham, NH.[99, 100] This paper described intense luminescence with a quantum efficiency of approximately 85% from GaAs junctions at 77°K. These results were so startling that they energized a number of research groups to consider the question of semiconductor lasers. These included research groups at General Electric, IBM, and MIT Lincoln Laboratories. (Notice that all of these groups achieved semiconductor laser operation in the latter half of 1962!)

The General Electric group used n-type GaAs wafers with a zinc diffusion to form a degenerate PN-junction. (The importance of the degenerate junction was pointed out by Bernard and Duraffourg in 1961.[101]) The resulting wafers were cut into strips approximately 0.5 mm wide and cemented to plates so that the edges could be lapped and polished. These polished edges formed the Fabry-Perot resonator structure. The resulting diodes were cooled to 77°K and operated in pulsed mode. The paper announcing the first semiconductor laser operation was the General Electric paper submitted in September 1962 and appearing in the November 1, 1962, edition of *Physical Review Letters*.[102]

---

[99]R. J. Keyes and T. M. Quist, "Recombination Radiation Emitted by Gallium Arsenide Diodes," presented at the *Solid State Device Res. Conf.*, 1962.

[100]The material in these papers was later published in R. J. Keyes and T. M. Quist, *Proc. IRE* 50:1822 (1962).

[101]M. G. A. Bernard and G. Duraffourg, *Phys. Stat. Sol.* 1:699 (1961).

[102]R. N. Hall, G. E. Fenner, J. D. Kingsley, T. J. Soltys, and R. O. Carlson, *Phys. Rev. Lett.* 9:366 (1962).

The IBM group also used n-type GaAs wafers with a zinc diffusion to form a degenerate PN-junction. The IBM group was struggling with the concept of how to make a resonator, and so decided to attempt to demonstrate stimulated emission without a resonator. The IBM *Applied Physics Letter* reporting the coherent stimulated emission from a GaAs PN-junction was submitted in October 1962, appearing within days of the publication of the General Electric *Physical Review Letter*.[103]

The MIT Lincoln Laboratories group also used n-type GaAs wafers with a zinc diffusion. They elected to use mechanical polishing to form the resonator structure and achieved laser action within a few weeks of the other groups. Their first paper was submitted in November 1962, and their results were reported in a pair of experimental and theoretical papers.[104, 105] The MIT Lincoln Laboratories group was also noteworthy for being the first group to address the question of applications for the new lasers by demonstrating TV transmission from a rooftop, and then from a nearby mountain top.[106]

Very shortly after the first demonstration of laser action in a degenerate GaAs PN-junction, a number of interesting and important advancements occurred. Just a few weeks after the initial announcement of GaAs diodes by the General Electric group,[107] Holonyak and Bevacqua demonstrated the first visible (710 nm) laser diode in GaAs$_{1-x}$P, using polished facets[108] (the Holonyak and Bevacqua paper was submitted in October 1962). The first cw operation (at 2°K) was observed by Howard et al.,[109] and the first pulsed room-temperature operation by Burns et al.[110]

The issue of polishing versus cleaving to create the small Fabry-Perot cavities was a critical one in early semiconductor laser development. Although cleaving is now considered to be somewhat easier than polishing, the first three lasers to be demonstrated all incorporated polished Fabry-Perot cavities. Holoyak originally attempted cleaving, but returned to polishing after difficulties in cleaving GaAs$_{1-x}$P. The first reported use of cleaving is by Bond et al. in 1963.[111] Dill and Rutz patented the cleaving concept from a disclosure filed on October 20, 1962.[112]

Laser research then began to diverge into a number of separate areas. The idea of using heterostructures in semiconductor diode lasers was a very powerful idea and was

[103]M. I. Nathan, W. P. Dumke, G. Burns, R. H. Dill, Jr., and G. Lasher, *Appl. Phys. Lett.* 1:62 (1962).

[104]T. M. Quist, R. H. Rediker, R. J. Keyes, W. E. Krag, B. Lax, A. L. McWhorter, and H. J. Zeiger, *Appl. Phys. Lett.* 1:91 (1962).

[105]A. L. McWhorter, H. J. Zeiger, and B. Lax, *J. Appl. Phys.* 34:235 (1963).

[106]R. H. Rediker, R. J. Keyes, T. M. Quist, M. J. Hudson, C. R. Grant, and R. G. Burgess, "Gallium Arsenide Diode Sends Television by Infrared Beam," *Electron.* 35: 44–45 (1962); and R. J. Keyes, T. M. Quist, R. H. Rediker, M. J. Hudson, C. R. Grant, and J. W. Meyer, "Modulated Infrared Diode Spans 30 Miles," *Electron.* 36: 38–39 (1963).

[107]R. N. Hall, G. E. Fenner, J. D. Kingsley, T. J. Soltys, and R. O. Carlson, *Phys. Rev. Lett.* 9:366 (1962).

[108]N. Holonyak, Jr., and S. F. Bevacqua, *Appl. Phys. Lett.* 1:82 (1962).

[109]W. E. Howard, F. F. Fang, F. H. Dill, Jr., and M. I. Nathan, *IBM J. Res. Develop.* 7:74 (1962).

[110]G. Burns and M. I. Nathan, *IBM J. Res. Develop.* 7:68 (1962).

[111]W. L. Bond, B. G. Cohen, R. C. C. Leite, and A. Yariv, *Appl. Phys. Lett.* 2:57 (1963).

[112]F. H. Dill, Jr., and R. F. Rutz, "Method of Fabrication of Crystalline Shapes," U.S. Patent #3,247,576, filed October 30, 1962; issued April 16, 1966.

first proposed by Kroemer in 1963.[113] However, the heterostructure concept required the development of appropriate materials-processing technologies, such as liquid phase epitaxy (LPE), metal-organic chemical vapor deposition (MOCVD), and molecular beam epitaxy (MBE). Therefore, the original proposal of Kroemer went relatively unnoticed.

In 1963, Nelson first demonstrated the liquid phase epitaxy growth of GaAs on GaAs.[114] In 1967, Woodall et al. demonstrated the growth of the heterostructure $Al_xGa_{1-x}As$ on GaAs.[115] The first LPE pulsed room temperature heterostructure lasers soon followed in 1969[116,117,118] and then cw room temperature heterostructure lasers.[119,120] Quantum confinement was the next major advancement in heterostructures. In 1978, Dupuis et al. first demonstrated a room-temperature quantum well laser.[121] Strained quantum well lasers soon followed.[122,123,124]

Distributed feedback lasers (DFB lasers) were another major track in laser development. DFB lasers incorporate an intrinsic grating to force single longitudinal mode operation. Kogelnik and Shank first developed the experimental and theoretical ideas behind DFB lasers.[125] Nakamura et al. reported the DFB semiconductor laser oscillation by photopumping GaAs.[126] Scifres et al.[127] reported the first AlGaAs/GaAs single heterostructure DFB junction lasers. Casey et al.[128] and Nakamura et al.[129] used an AlGaAs/GaAs separately confined heterostructure to achieve the first DFB cw oscillation at room temperature. Room-temperature cw operation of a DFB laser at the fiber-optical communication wavelength of 1.5 μm in InGaAsP/InP was first reported by Utaka et al.[130]

Distributed Bragg reflector lasers (DBR lasers) are a variation on DFB lasers where the reflectors are outside (rather than inside) the active region. Lasing occurs between the

[113]H. Kroemer, *Proc. IEEE* 51:1782 (1963).

[114]H. Nelson, *RCA Rev.* 24:603 (1963).

[115]J. M. Woodall, H. Rupprecht, and G. D. Pettit, *Solid-State Device Conf.*, 1967. Abstracts reported in *IEEE Trans. Electron. Devices* ED-14:630 (1967).

[116]H. Kressel and H. Nelson, *RCA Rev.* 30:106 (1969).

[117]I. Hayashi, M. B. Panish, and P. W. Foy, *IEEE J. Quantum Electron.* QE-5:211 (1969).

[118]Zh. I. Alferov, V. M. Andreev, E. L. Portnoi, and M. K. Trukan, *Fiz. Tekh. Poluprovodn.* 3:1328 (1969) [*Sov. Phys. Semicond.* 3:1107 (1970)].

[119]I. Hayashi, M. B. Panish, P. W. Foy, and S. Sumuski, *Appl. Phys. Lett.* 17:109 (1970).

[120]Zh. I. Alferov, V. M. Andreev, D. Z. Garbuzov, Yu. V. Zhilyaev, E. P. Morozov, E. L. Portnoi, and V. G. Trofim, *Fiz. Tekh. Poluprovodn.* 4:1826 (1970). [*Sov. Phys. Semicond.* 4:1573 (1971)].

[121]D. Dupuis, R. D. Dapkus, N. Holonyak, Jr., E. A. Rezek, and R. Chin, *Appl. Phys. Lett.* 32:295 (1978).

[122]E. Yablonovitch and E. O. Kane, *J. Lightwave Technol.* LT-4:504 (1986); 6:1292 (1988).

[123]D. P. Bour, D. B. Gilbert, L. Elbaum, and M. G. Harvey, *Appl. Phys. Lett.* 53:2371 (1988).

[124]P. J. A. Thijs and T. van Dongen, *Electron. Lett.* 25:1735 (1989).

[125]H. Kogelnik and C. V. Shank, *Appl. Phys. Lett.* 18:152 (1971); and H. Kogelnik and C. V. Shank, *Appl. Phys. Lett.* 43:2327 (1972).

[126]M. Nakamura, A. Yariv, H. W. Yen, and S. Somekh, *Appl. Phys. Lett.* 22:515 (1973).

[127]D. R. Scifres, R. D. Burnham, and W. Streifer, *Appl. Phys. Lett.* 25:203 (1974).

[128]H. C. Casey, Jr., S. Somekh, and M. Ilegems, *Appl. Phys. Lett.* 27:142 (1975).

[129]M. Nakamura, A. Aiki, J. Umeda, and A. Yariv, *Appl. Phys. Lett.* 27:403 (1975).

[130]K. Utaka, S. Akiba, K. Sakai, and Y. Matsushima, *Electron. Lett.* 17:961 (1981).

grating mirrors, or between one grating and a conventional facet. The first DBR laser was an AlGaAs/GaAs laser demonstrated by Reinhart et al.[131]

Vertical-cavity surface-emitting lasers (VCSEL) were later developments in semiconductor laser technology.[132] Soda et al. demonstrated the first VCSEL.[133] This was a double heterostructure InGaAsP device operating at 1.3 μm. It used metal mirrors and lased at 77°K. In 1982, Burnham, Scifres and Streifer filed a patent on various designs for VCSEL devices.[134] Epitaxial mirrors for VCSEL devices were first demonstrated in 1983.[135] In 1989, the first cw room temperature VCSEL device was demonstrated by Jewell et al.[136] This device was an quantum well active region sandwiched between n- and p-doped semiconductor Bragg reflectors.

Historical details of this era from the perspective of the major participants are available in a series of review papers in volume QE-23 of the *IEEE Journal of Quantum Electronics*.[137] Additional historical details can be found in the reviews by Hall,[138] Rediker,[139] and in the books by Kressel and Butler,[140] and by Casey and Panish.[141] IEEE has also published a summary of seminal papers on semiconductor diode lasers.[142]

12.3.2 The Basics of the Semiconductor Diode Laser

Energy band structure.   The semiconductor laser can be modeled as a two-level laser system. The upper laser state is the conduction band, and the lower laser state is the valence band. The laser wavelength is emitted at the bandgap of the semiconductor.

In order for the semiconductor to have sufficient gain to operate as a laser, it is usually necessary for the electron transition from the conduction band to the valence band to be a direct radiative transition. Gallium arsenide (GaAs) is an example of a direct semiconductor. Silicon is an example of an indirect semiconductor. The distinction between a direct and indirect semiconductor material is often explained using the E (energy) versus k (momentum)

---

[131]F. K. Reinhart, R. A. Logan, and C. V. Shank, *Appl. Phys. Lett.* 27:45 (1975).

[132]J. Jewell, *Scientific American* November: 86–94 (1991).

[133]H. Soda, K. Iga, C. Yitahara, and Y. Suematsu, *Jpn. J. Appl. Phys.* 18:2329 (1979).

[134]R. Burnham, D. R. Scifres, and W. Streifer, U.S. Patent #4,309,670, Jan. 1982.

[135]A. Chailertvanitkul, S. Uchiyama, Y. Kotaki, Y. Kokubun, and K. Iga, *Annual Meet. Jpn. Sec. Appl. Phys.* (1983).

[136]J. L. Jewell, A. Scherer, S. L. McCall, Y. H. Lee, S. Walker, J. P. Harbison, and L. T. Florez, *Electron. Lett.* 25:1123 (1989).

[137]R. N. Hall, *IEEE J. of Quantum Electron.* QE-23:674 (1987); M. I. Nathan, *IEEE J. of Quantum Electron.* QE-23:679 (1987); N. Holonyak, *IEEE J. of Quantum Electron.* QE-23:684 (1987), and R. H. Rediker, *IEEE J. of Quantum Electron.* QE-23:692 (1987).

[138]R. N. Hall, "Injection lasers," *IEEE Trans. Electron Dev.* ED-23:700 (1976).

[139]R. H. Rediker, I. Melngailis, and A. Mooradian, "Lasers, Their Development and Applications at M.I.T. Lincoln Laboratory," *IEEE J. Quantum Electron.* QE-20:602 (1984).

[140]H. Kressel and J. K. Butler, *Semiconductor Lasers and Heterojunction LEDs* (New York: Academic Press, 1977).

[141]H. C. Casey, Jr., and M. B. Panish, *Heterostructure Lasers, Parts A and B* (New York: Academic Press, 1978).

[142]W. Streifer and M. Ettenberg, eds, *Semiconductor Diode Lasers* (New York: IEEE Press, 1991).
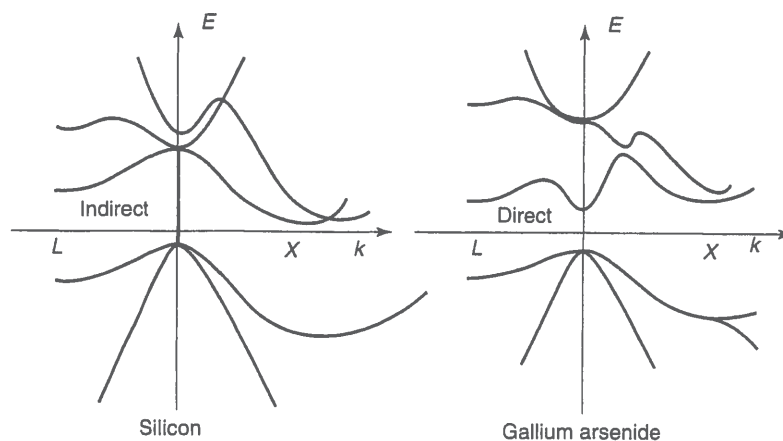
Figure 12.31   The distinction between a direct and indirect semiconductor material is often explained using the E (energy) versus k (momentum) diagram for the semiconductor. If the minima of the conduction band and the maxima of the valence band both occur at $k = 0$, then the semiconductor is direct. If the minima and maxima do not overlap at all, or overlap at $k \neq 0$, then the semiconductor is indirect.

diagram for the semiconductor. If the minima of the conduction band and the maxima of the valence band both occur at $k = 0$, then the semiconductor is direct. If the minima and maxima do not overlap at all or overlap at $k \neq 0$, then the semiconductor is indirect. Examples of E versus k diagrams for indirect and direct materials are given in Figure 12.31.

Pumping the semiconductor diode laser.   In order for the semiconductor to lase, it is necessary to create a population inversion between the valence and the conduction bands. Such a population inversion can be created by external pumping (lasers, electron beams, or flashlamps) or by internally pumping (with a PN-junction).

The simplest way to create a population inversion is to pump the semiconductor with another light source. This technique is termed photopumping and is commonly used to test new semiconductor laser materials in order to determine their suitability for laser operation. One way to photopump a semiconductor laser is to use a conventional gas laser source (such as a HeNe or an argon-ion) as a pump source. This has the advantage of simplicity, but tends to overheat the laser material. For this reason, photopumped laser slices are generally thinned and mounted in thermally conductive holders. Another way to photopump is to use a conventional pulsed laser source (such as a Nd:YAG or glass laser). This not only solves the thermal problems, but also permits testing of recombination rates in the material. A very clever way to photopump a diode laser material is with another diode laser. The sample is thinned and mounted directly on the output window of the diode laser. Although the actual diode laser power is relatively small, the coupling efficiency between the diode laser and the photopumped laser is excellent.

However, the majority of commercial semiconductor lasers are electrically pumped using a PN-junction. Under conditions of high current injection in a PN-junction, a re-
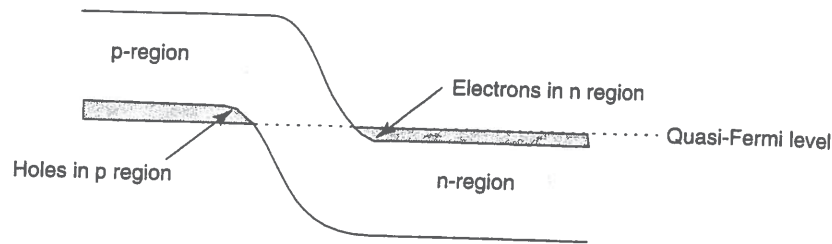
Figure 12.32   In equilibrium, the quasi-Fermi levels of the degenerate p- and n-junction laser material align.
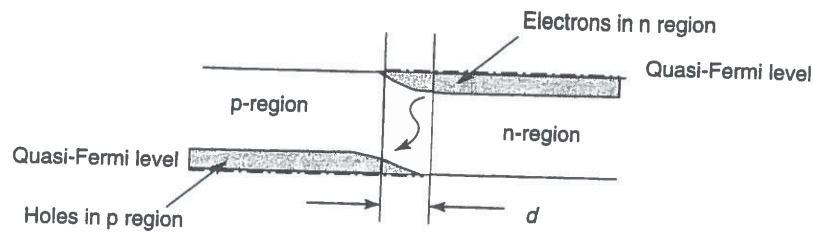

Figure 12.33   The quasi-Fermi levels will misalign by the value of the applied voltage. Under the influence of the forward bias, the holes will drift to the n-region and the electrons will drift into the p-region. The holes and electrons are now spatially coincident and hole-electron recombination occurs.

gion near the depletion region will contain an inverted population of electrons and holes. Appropriate alignment of this region with the cleaved facets will result in laser operation.

Consider the energy band diagram for a simple PN-junction intended for use in a semiconductor photon source. Initially, one side of the junction is heavily doped n and the other side is heavily doped p. In general, both materials are doped degenerately (meaning that the quasi-Fermi level is above the bandedge). In equilibrium the quasi-Fermi levels align as shown in Figure 12.32.

When a positive voltage is applied to the p-region and a negative voltage is applied to the n-region, then the diode is forward biased. The quasi-Fermi levels will misalign by the value of the applied voltage. Under the influence of the forward bias, the holes will drift to the n-region and the electrons will drift into the p-region. The holes and electrons are now spatially coincident and hole-electron recombination occurs (see Figure 12.33).

Notice that in the nonequilibrium situation, the quasi-Fermi levels for the electrons and holes have separated. The spatial distance between the quasi-Fermi levels is essentially the depth d of the active region. In III-V semiconductors (the most common semiconductors for commercial laser diodes), the electrons are much more mobile than the holes. Therefore, the depth of the active region is principally determined by the mobility of the electrons. This distance is approximately given by

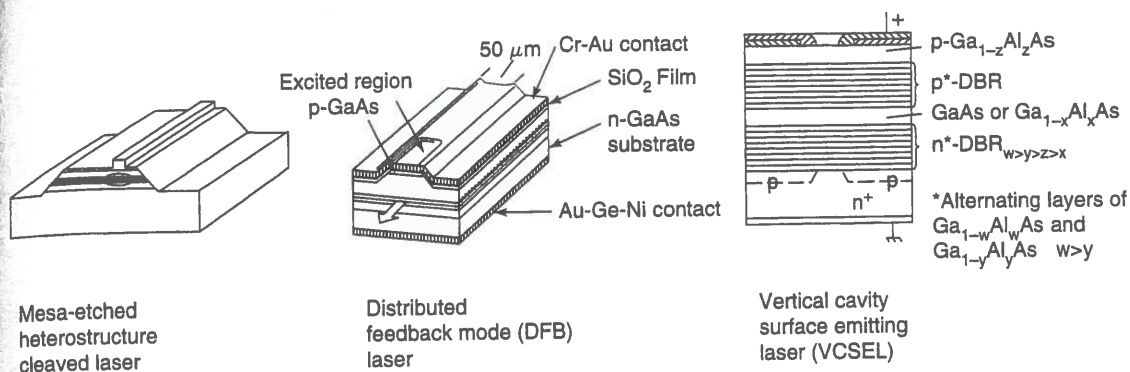$$d = \sqrt{D_n \tau_n} = \sqrt{\frac{D_n n_p}{dn_p/dt}}$$

Figure 12.34 A few of the possible semiconductor laser resonator structures: DFB is from K. Aiki, M. Nakamura, and J. Umeda, "Schematic Structure of a GaAlAs/GaAS Distributed Feedback Laser," *IEEE J. of Quantum Electron.* QE-12:597 (1976), ©1976 IEEE; VCSEL is from R. Burnham, D.R. Scifres, and W. Streifer, U.S. Patent #4,309,670 (1982).

where n_p is the electron concentration in the p-region and D_n is the diffusion constant for electrons. Typical numbers for d are on the order of 1 μm. (Again, notice that this is on the order of the same size as the wavelength of the electromagnetic mode being amplified.)

Creating the semiconductor diode laser resonator.   There are an astonishing number of possible forms for the semiconductor laser resonator (see Figure 12.34).

In the simplest form, a semiconductor laser consists of small rectangular slab of semiconductor material with two polished or cleaved facets to act as resonator mirrors. The other facets are destroyed in some way (etched, ground, sawn, ion implanted, etc.) in order to avoid spurious laser modes.

The typical horizontal cleaved laser construction can be modified in a number of ways. For example, the facets can be etched using wet or dry processing techniques. External mirrors, gratings, or combinations of mirrors and gratings can be used in place of cleaved facets. External elements can be incorporated off-chip or integrated into the chip.

Semiconductor lasers can be fabricated to lase vertically. With this type of construction, reflecting layers are fabricated on the substrate and the laser operates perpendicularly to the substrate. Reflecting layers can be made from metal, dielectric films, and semiconductor multilayers. Such lasers are called VCSEL.

It is also possible to incorporate gratings directly into the laser design. This results in a laser with a single longitudinal mode forced by distributed feedback from the internal grating. Such lasers are termed DFB lasers. In DBR lasers, a variation on DFB lasers, lasing occurs between the grating mirrors, or between one grating and a conventional facet.

Light propagation in the semiconductor diode laser.   In a laser diode, the photons must be modeled as collective entities traveling in a confined fashion down a waveguide. This gives a different character to the issue of modeling light output from a laser diode as compared to a conventional laser. In general, the far-field pattern from a laser diode is determined by the Fourier integral of the electromagnetic field propagating in the waveguide. The electromagnetic field within the waveguide can be calculated using

the eigenvalue equations for wave propagation in a slab waveguide (for example, see Casey and Panish[143]).

Homostructure semiconductor diode lasers, heterostructure semiconductor diode lasers, and the importance of lattice matching.   Early semiconductor lasers were constructed from n- and p-type layers of the same semiconductor material. Such lasers are called homostructure lasers. Homostructure lasers have the advantage of structural simplicity.

However, semiconductor lasers can also be constructed from n- and p- type layers of different semiconductor materials. Such lasers are called heterostructure lasers. The energy band structure and index of refraction profiles of heterostructure lasers can be tailored to meet a given application.

The majority of commercial heterostructure semiconductor lasers are fabricated from semiconductor materials in columns III and V of the periodic table. [Column III is boron (B), aluminum (Al), gallium (Ga), indium (In), and thallium (Tl); column V is nitrogen (N), phosphorus (P), arsenic (As), antimony (Sb), and bismuth (Bi).] Common laser materials include virtually all combinations of Al, Ga, and In, with P and As. Some work has been done with B, Al, and Ga, with N; as well as Al, Ga, and In with Sb. Very little has been done with Tl and Bi.

Heterostructure lasers require layering these different materials. This is a very complex problem, as the materials have different physical properties. Perhaps the most important of these properties is the lattice spacing. If the materials do not have the same lattice spacing, then dislocations can appear in the semiconductor laser. In addition to the structural difficulties imposed by dislocations, dislocations can also be highly detrimental to semiconductor laser operation as they can serve as a nonradiative sink for carriers.

A very useful diagram for visualizing lattice match in heterostructure lasers is the energy versus lattice constant diagram. (An example of such a diagram for III-V materials is given in Figure 12.35). Notice that only the AlAs-GaAs system is lattice-matched across the entire compositional range. This is one major reason for the widespread use of AlGaAs/GaAs heterostructures on GaAs substrates for semiconductor laser diodes.

12.3.3 Confinement in the Semiconductor Diode Laser

Since the electromagnetic mode in semiconductor lasers is on the order of the size of the laser device, then horizontal and vertical confinement are important issues in semiconductor laser design. These issues usually do not arise in conventional laser design, as conventional lasers are typically operating in a propagation mode where the wavelength is much smaller than the resonator dimensions.

Vertical confinement.   Typically vertical confinement is provided by creating material combinations with index of refraction profiles that confine the optical wave. Some of these combinations offer the additional advantage of confining the carriers as well.

---

[143]H. C. Casey, Jr., and M. B. Panish, *Heterostructure Lasers, Parts A and B* (New York: Academic Press, 1978), Chapter 2.
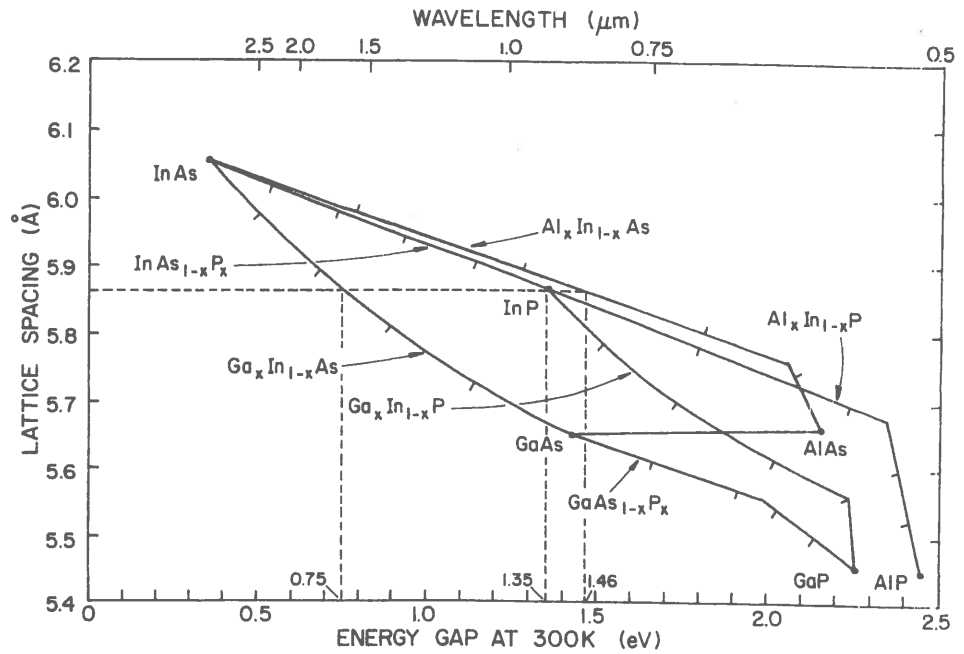
Figure 12.35   The energy versus lattice constant diagram is very useful for visualizing lattice match in heterostructure lasers. (From E. C. H. Parker, *Physics of Molecular Beam Epitaxy* (New York: Plenum Press, 1985), p. 277, Figure 2. Copyright Plenum Press.)
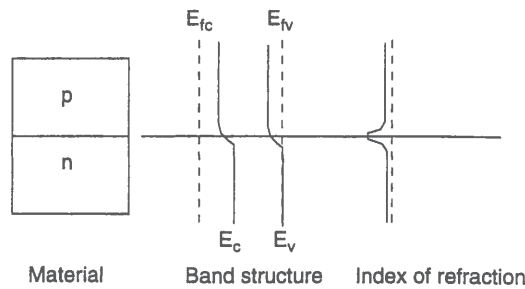

Figure 12.36   A typical homostructure laser consists of one material type with degenerately doped p and n regions. There is only a slight refractive index change at the n-junction to assist in vertical optical confinement of the laser beam.

Homostructure lasers were the very first type of semiconductor laser structure demonstrated. A typical homostructure laser (see Figure 12.36) consists of one material type (for example, GaAs) with degenerately doped p and n regions. There is only a slight refractive index change at the n-junction to assist in vertical optical confinement of the laser beam. Homostructure lasers offer the advantages of simplicity, but the disadvantages of poor confinement.

Single heterostructure lasers were the first type of semiconductor heterostructure laser developed. A typical single heterostructure GaAs laser (see Figure 12.37) is composed of a homojunction GaAs laser diode followed by a p-type AlGaAs layer (with a larger bandgap and lower index of refraction). This geometry creates an index of refraction bump

in the p-type GaAs layer. The index of refraction bump provides some vertical confinement for the laser action occurring in the p-type GaAs. Single heterostructure lasers provide significantly more vertical confinement than homostructure lasers, but require more complex heterostructure growth processes.
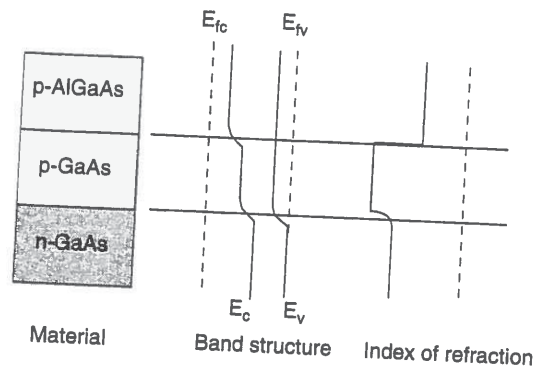

Figure 12.37   A typical single heterostructure laser is composed of a homojunction laser diode followed by a p-type layer with a larger bandgap and lower index of refraction. This geometry creates an index of refraction bump in the p-type GaAs layer. The index of refraction bump provides some vertical confinement for the laser action.

Double heterostructure (DH) lasers have become the standard heterostructure laser type. A typical DH GaAs laser (see Figure 12.38) is composed of a p-type GaAs layer sandwiched between n-type and p-type AlGaAs layers. This geometry creates a large index of refraction bump in the p-type GaAs layer. The index of refraction bump provides vertical confinement for the laser action occurring in the p-type GaAs. DH lasers offer a very nice compromise between the advantages of an index guiding vertical confinement layer, and the disadvantages of heterostructure laser growth.

GRINSCH (graded-index separate confinement heterostructure) lasers offer both optical and electrical confinement in an effort to achieve lower thresholds and narrower beam patterns. A GRINSCH laser is basically a DH laser, but one where the AlGaAs layer has been graded down to meet the GaAs layer (see Figure 12.39). This provides both electron confinement (from the energetic well created by the graded bandgap) and optical confinement (from the index of refraction bump between the AlGaAs and GaAs materials).

GRINSCH lasers frequently find application as quantum well lasers, because the graded bandgap provides a good "funnel" to confine the electrons to the the quantum well regions (see Figure 12.40). MQW-GRINSCH lasers are very popular geometries as they combine many of the best features of DH lasers and quantum wells.

Horizontal confinement.   For many semiconductor laser diode applications it is necessary to confine the carriers both in the horizontal and vertical directions. The most popular method for horizontal confinement is to restrict the size of the gain region, a method called *gain confinement*. There are a large number of gain confinement techniques, but the most popular tend to fall into the categories of contact stripe, mesa etch, ion-implantation methods, and regrowth techniques (such as buried heterostructures).

In the contact stripe method, the gain confinement is provided by restricting the spatial extent of the metal contact (see Figure 12.41). This method offers processing simplicity, but provides relatively poor confinement due to electron transport underneath the stripe.
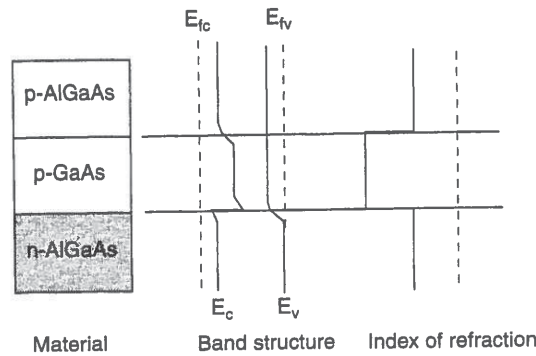
Figure 12.38   A typical double heterostructure laser is composed of a p-type lower bandgap layer sandwiched between n-type and p-type higher bandgap layers. This geometry creates a large index of refraction bump in the p-type layer. The index of refraction bump provides vertical confinement for the laser action occuring in the p-type layer.
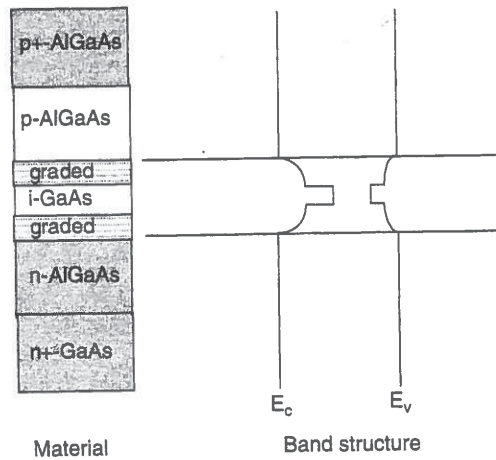

Figure 12.39   A GRINSCH laser is basically a DH laser, but one where the higher bandgap layer has been graded down to meet the lower bandgap layer. This provides both electron confinement (from the energetic well created by the graded bandgap) and optical confinement (from the index of refraction bump between the high and low index materials).

In the mesa etch method, the gain confinement is provided by etching one or several layers of the structure (see Figure 12.42). This method is more difficult to process (as it is both highly nonplanar and requires a sensitive etch stop), but it offers significantly better confinement than the contact stripe method.

In the ion-implantation method, ions are implanted in regions other than the region of interest (see Figure 12.43). This method offers process simplicity and provides a good quality output beam.

In the buried heterostructure method, the gain region is surrounded in both the vertical and horizontal directions by a waveguide of material (see Figure 12.44). Thus, the buried heterostructure process is a two-part method. First, an initial set of layers is grown in an epitaxial system. Then, the wafer is removed from the epitaxial growth system, processed, and returned to the system for new layers to be grown on the material. This process provides outstanding confinement, as the laser is essentially operating in a square waveguide. However, the two-part process cycle is exceptionally complex.
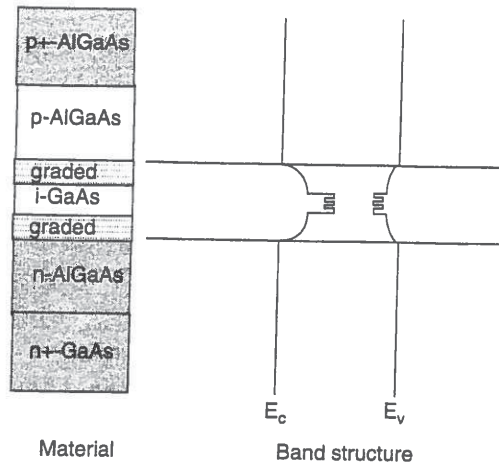
Material   Band structure

Figure 12.40   GRINSCH lasers frequently find application as quantum well lasers, because the graded bandgap provides a good "funnel" to confine the electrons to the quantum well regions.
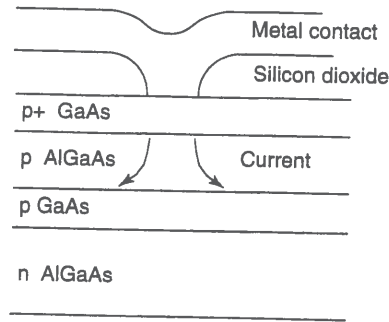

Figure 12.41   In the contact stripe method, the gain confinement is provided by restricting the spatial extent of the metal contact.
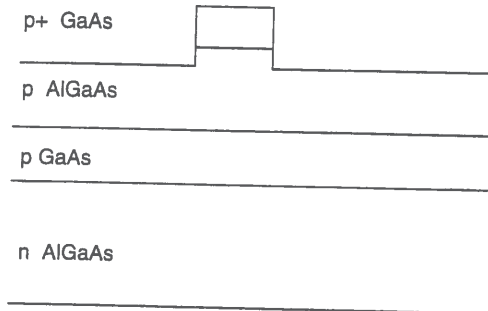

Figure 12.42   In the mesa etch method, the gain confinement is provided by etching one or several layers of the structure.

12.3.4 The Quantum Well Semiconductor Diode Laser

A quantum well is a heterostructure composed of two materials of differing bandgap. The two materials are fabricated in a sandwich with the higher bandgap material forming the outside (or barrier) and the lower bandgap material forming the inside (or well). Under these conditions, energy wells are created in both the conduction and valence bands of the heterostructure (see Figure 12.45).

Discrete quantum states (similar to states in a hydrogen atom) will form in the conduction and valence wells (see Figure 12.46). As with a hydrogen atom, electrons transitioning between these states will produce photons possessing the difference energy between the states.

However, unlike a hydrogen atom, the energy of these quantum well states is a function of the width of the quantum wells. The narrower the quantum well, the larger the resulting transitional energy (to the eventual limit that the transition energy between the first valence and first conduction band state matches the energy gap of the barrier material). The wider the quantum well, the smaller the resulting transitional energy (to the eventual limit that the transition energy between the first valence and first conduction band state matches the energy gap of the well material).

In engineering practice, quantum wells provide the means to manufacture semiconductor lasers at any wavelength between that of the barrier material and the well material. In addition, quantum well lasers provide lower lasing thresholds and higher differential quantum efficiencies than equivalent DH lasers.
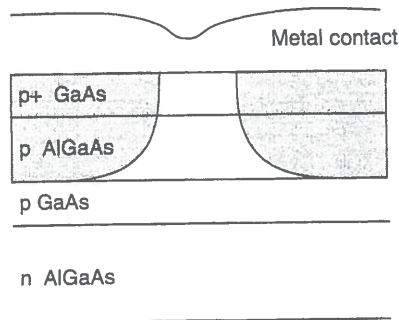

Figure 12.43   In the ion-implantation method, ions are implanted in regions other than the region of interest.
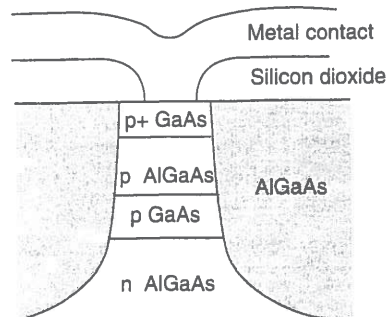

Figure 12.44   In the buried heterostructure method, the gain region is surrounded in both the vertical and horizontal directions by a waveguide of material.
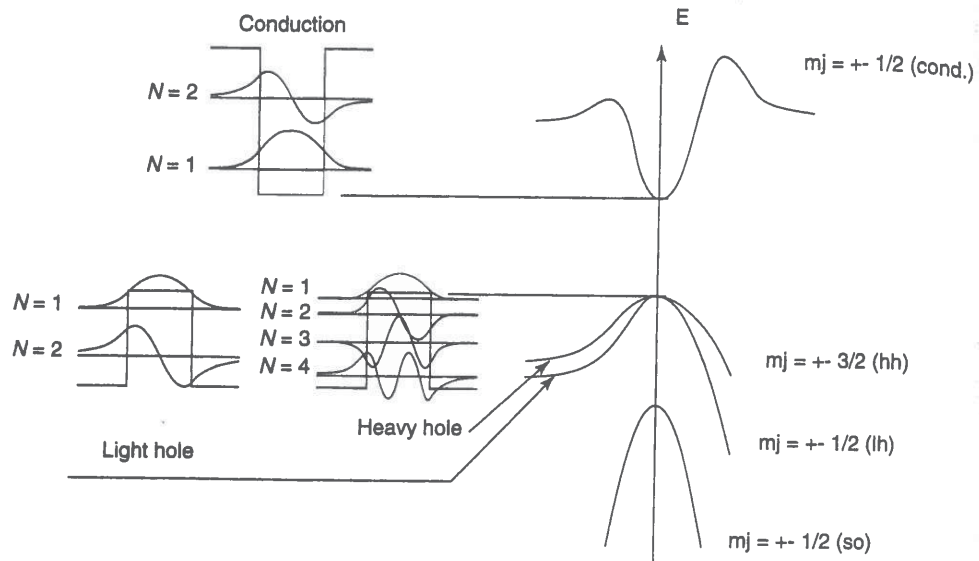
Figure 12.45 A quantum well is a heterostructure composed of two materials of differing bandgap. Under these conditions, energy wells are created in both the conduction and valence bands of the heterostructure.
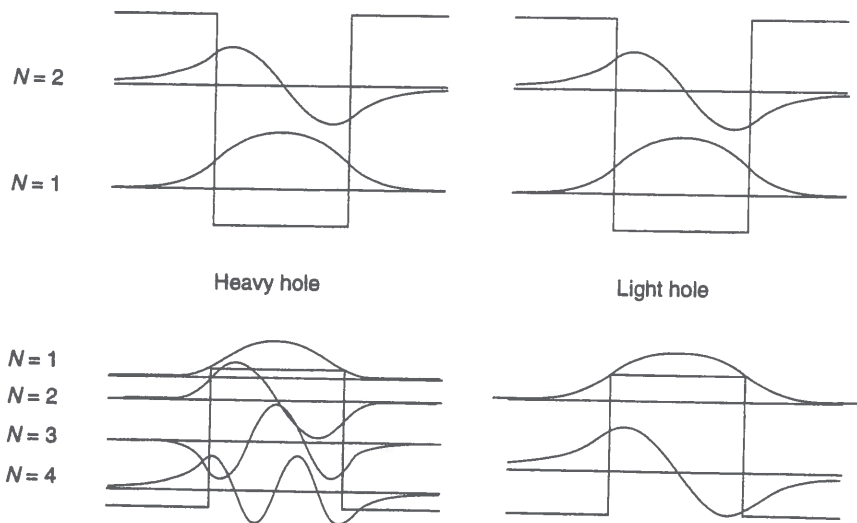

Figure 12.46 Discrete quantum states (similar to states in a hydrogen atom) will form in the conduction and valence wells of a quantum well material.
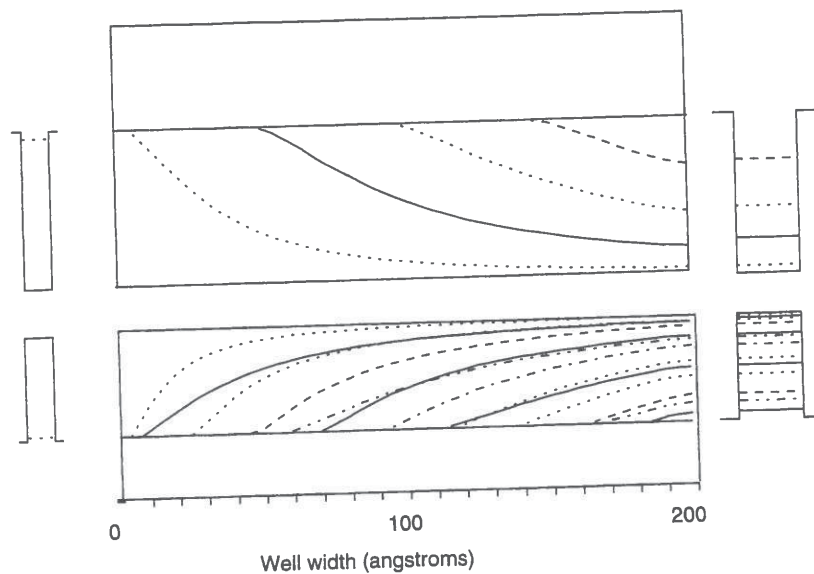
Figure 12.47 The narrower the quantum well, the larger the resulting transitional energy (to the eventual limit that the transition energy between the first valence and first conduction band state matches the energy gap of the barrier material). The wider the quantum well, the smaller the resulting transitional energy (to the eventual limit that the transition energy between the first valence and first conduction band state matches the energy gap of the well material).

12.3.5 Application Highlight: The CD Player

Introduction to the CD audio player.   The CD audio player (and its close relative, the CD ROM) are probably the most widely known applications of laser diodes.

A CD disk contains a long string of pits written helically on tracks on the disk. Each pit is approximately 0.5 μm wide and 0.83 μm to 3.56 μm long. Each track is separated from the next track by 1.6 μm. The CD disk is actually read from the bottom. Thus, from the viewpoint of the laser beam reading the disk, the "pit" in the CD is actually a "bump." Interestingly enough, the *edges* of each pit (rather than the pit itself) correspond to binary ones. The signal has been encoded to ensure that there are no adjacent ones. (See Figure 12.48.)

The polycarbonate disk itself is part of the optical system for reading the pits (see Figure 12.49). The index of refraction of air is 1.0 while the index of refraction of the polycarbonate is 1.55. Laser light incident on the polycarbonate surface will be refracted at a greater angle into the surface. Thus, the original incident spot of around 800 μm (entering the polycarbonate) will be focused down to about 1.7 μm (at the metal surface). This helps to minimize the effect of dust and scratches on the surface.

The laser used for the CD player is typically an AlGaAs laser diode with a wavelength (in air) of 780 nm. The wavelength inside the polycarbonate is a factor of $n = 1.55$ smaller (about 500 nm). The pit/bump is carefully fabricated so that it is a quarter-wavelength high (notice a wavelength *inside* the polycarbonate). Light striking the land travels 1/4 + 1/4 =
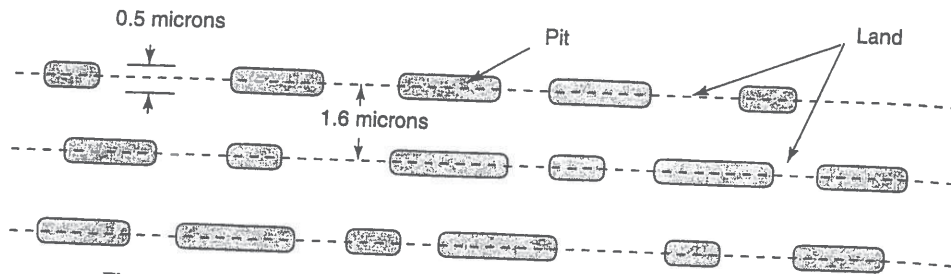
0.5 microns

Pit

Land

1.6 microns

Figure 12.48 A CD disk contains a long string of pits written helically on tracks on the disk. Each pit is approximately 0.5 microns wide and 0.83 microns to 3.56 microns long.
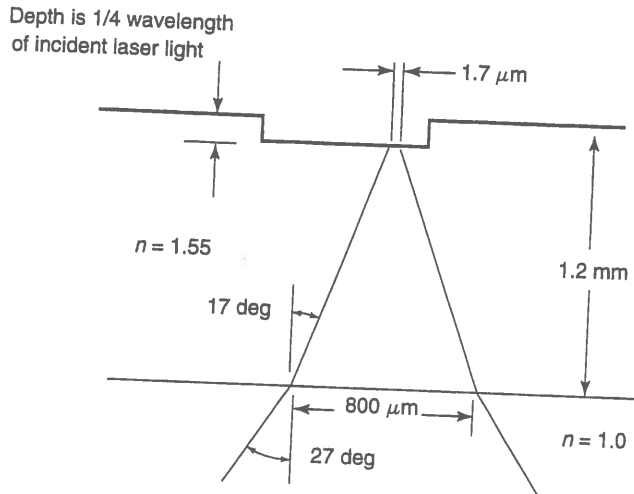
Depth is 1/4 wavelength
of incident laser light

1.7 μm

$n = 1.55$

1.2 mm

17 deg

800 μm

27 deg

$n = 1.0$

Figure 12.49 The polycarbonate disk is part of the optical system for reading the pits. The original incident spot of around 800 microns (entering the polycarbonate) will be focused down to about 1.7 microns (at the metal surface). This helps to minimize the effect of dust and scratches on the surface.

1/2 of a wavelength further than light striking the top of the pit. The light reflected from the land is then delayed by 1/2 wavelength, and so is exactly out-of-phase with the light reflected from the pit. Thus, these two waves will interfere destructively.

The spacing between pits is also carefully selected. Recall that the image of a beam passing through a round aperture will form a characteristic pattern called an Airy disk. The FWHM center of the Airy disk pattern is a spot about 1.7 μm wide and falls neatly on top of the pit track. The nulls in the Airy pattern are carefully situated to fall on the neighboring pit tracks. This minimizes crosstalk from neighboring pits.

The three-beam optical train.   The most common optical train in modern CD players is the three-beam optical train (see Figure 12.50).

The basic operation of the optical train relies on the polarization properties of light. Light is emitted by the laser diode and enters a diffraction grating. The grating converts the light into a central peak plus side peaks. (The main central peak and two side peaks are important in the tracking mechanism.) The three beams go through a polarizing beam splitter. This only transmits polarizations parallel to the page. The emerging light (now polarized parallel to the page) is collimated. The collimated light goes through a quarter-
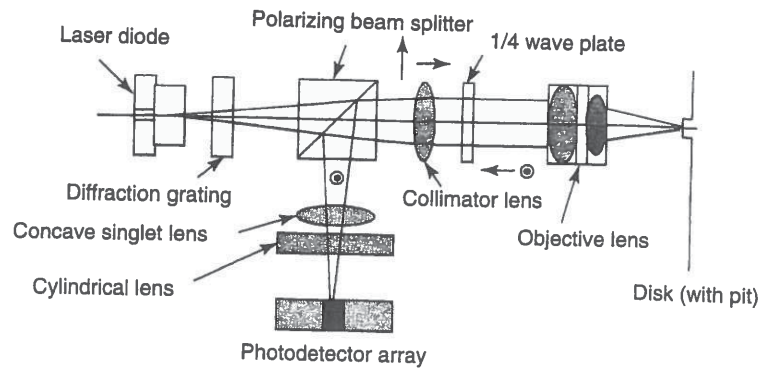
Figure 12.50   The most common optical train in modern CD players is the three-beam optical train.

wave plate and is converted into circularly polarized light. The circularly polarized light is then focused down onto the disk. If the light strikes land, it is reflected back into the objective lens; if the light strikes the pit, it is not reflected. The light then passes through the quarter wave plate again and emerges polarized perpendicular to the original beam (in other words, the light polarization is now vertical with respect to the paper). When the vertically polarized light hits the polarizing beam splitter this time, it will be reflected (not transmitted as before). Thus, it will reflect though the focusing lens and then the cylindrical lens and be imaged on the photodetector array.

Three-beam autofocus.   The separation between the laser and the compact disk is critical for the correct operation of the CD player. A clever astigmatic autofocus mechanism is used to maintain this distance. This autofocus mechanism incorporates a cylindrical lens immediately in front of the photodetector array (see Figure 12.51).

If the objective lens is closer to the compact disk than the focal length of the object lens, then the cylindrical lens creates an elliptical image on the photodetector array. If the objective lens is further away from the compact disk than the focal length of the object lens, then the cylindrical lens again creates an elliptical image on the photodetector array. However, this elliptical image is perpendicular to first image. (Of course, if the disk is right at the focal length of the objective lens, then the cylindrical lens does not affect the image and it is perfectly circular.)

So, if the disk is too far away, quadrants D and B will get more light quadrants A and C (see Figure 12.52). Similarly, if the disk is too close, quadrants A and C will get more light than D and B. If things are just right, then all quadrants will get the same amount of light. So, it is possible to build a simple circuit that will maintain the object lens at just the right distance from the disk.

Three-beam tracking.   Maintaining the laser beam on the track is also critical for the correct operation of the CD player. The three-beam optical train uses three separate beams to maintain the tracking. These beams are created by the diffraction grating (see Figure 12.53). When the laser beam goes through the diffraction grating, it is split up into a
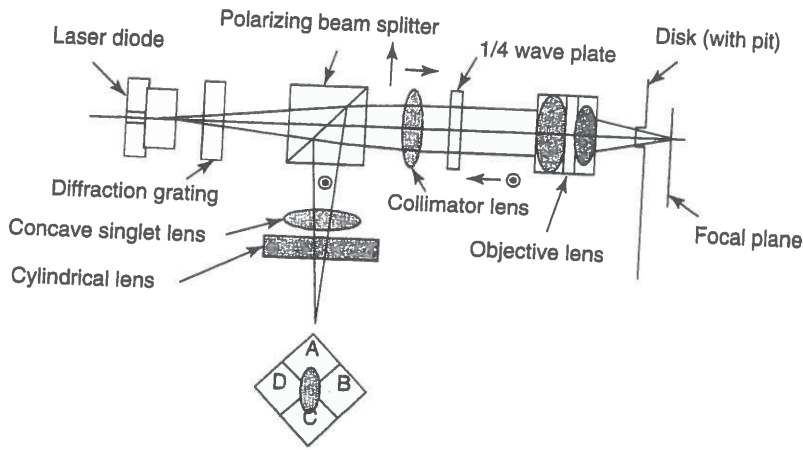
Figure 12.51 The separation between the laser and the compact disk is critical for the correct operation of the CD player. A clever astigmatic autofocus mechanism is used to maintain this distance.

Too far   Just right   Too close

Figure 12.52 If the objective lens is closer to the compact disk than the focal length of the object lens, then the cylindrical lens creates an elliptical image on the photodetector array.
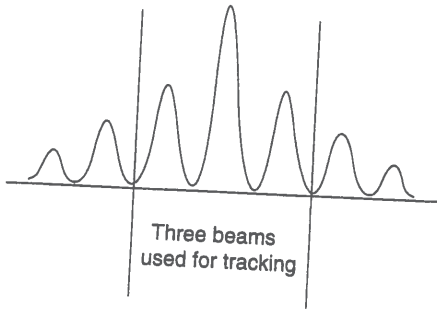

Three beams used for tracking

Figure 12.53 The three-beam optical train uses three separate beams to keep the laser beam on the track. These beams are created by the diffraction grating.

central bright beam plus a number of side beams. The central beam and one beam on each side are used by the CD for the tracking system.

To appreciate the tracking mechanism, consider a segment of the CD player containing several tracks (see Figure 12.54). If the optical head is on track, then the primary beam will be centered on a track (with pits and bumps) and the two secondary beams will be centered on land. (The three spots are deliberately offset approximately 20 microns with respect to each other to avoid crosstalk.)

Two additional detectors are placed alongside the main quadrant detector in order to pick up these subsidiary beams. If the three beams are on track, then the two subsidiary photodetectors have equal amounts of light and will be quite bright because they are only
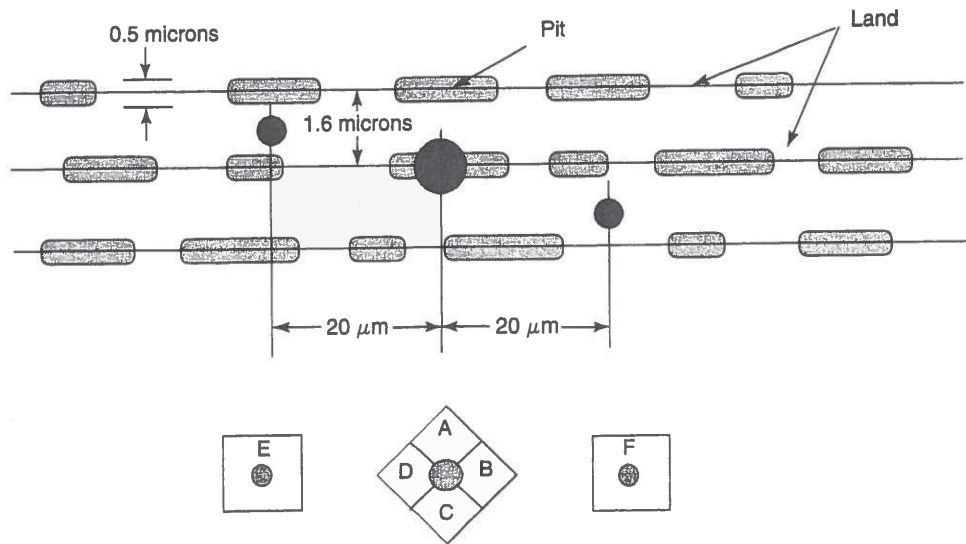
Figure 12.54 If the optical head is on track, then the primary beam will be centered on a track (with pits and bumps) and the two secondary beams will be centered on land.
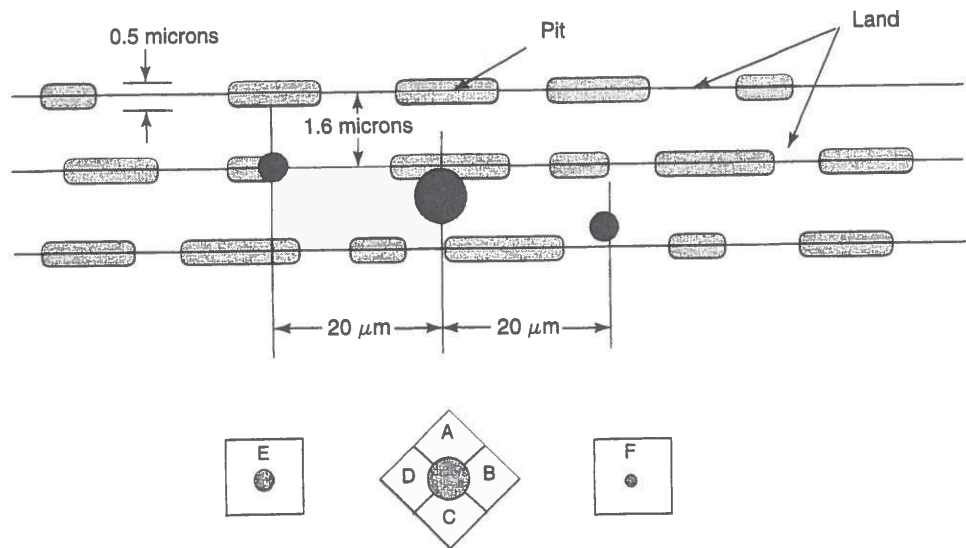

Figure 12.55 If the optical head is off track, then the center spot gets more light energy (because there are fewer pits off track) and the side detectors will be misbalanced.

tracking on land. The central beam will be reduced in brightness because it is tracking on both land and pits (see Figure 12.54). However, if the optical head is off track, then the center spot gets more light (because there are fewer pits off track) and the side detectors will be misbalanced (see Figure 12.55).

Additional optical storage applications using lasers. The CD audio player is just one of many optical storage applications using lasers. The CD recordable (CD-R) is another technology advancement in the optical storage area. The CD-R uses a laser beam to interact with a nonlinear dye and "write" pits in the CD-R disk. CD-R disks are "write once" devices, but offer exceptional performance for archival applications. (This textbook was delivered to the publisher on a CD-R disk.)

Magneto-optical storage is another fascinating laser diode application. Magneto-optical systems use a laser beam to change the orientation of a magnetic material. The process requires heating the magnetic material to near its Curie temperature and using the focused field of the laser to localize the change. The resulting magnetic spots are read optically using either the Kerr or the Faraday effect.

Another optical storage application that is just achieving success in the commercial marketplace is the DVD or digital video disk player. A combination of CD laser technology and clever digital algorithms has resulted in a more robust alternative to the video tape machine.